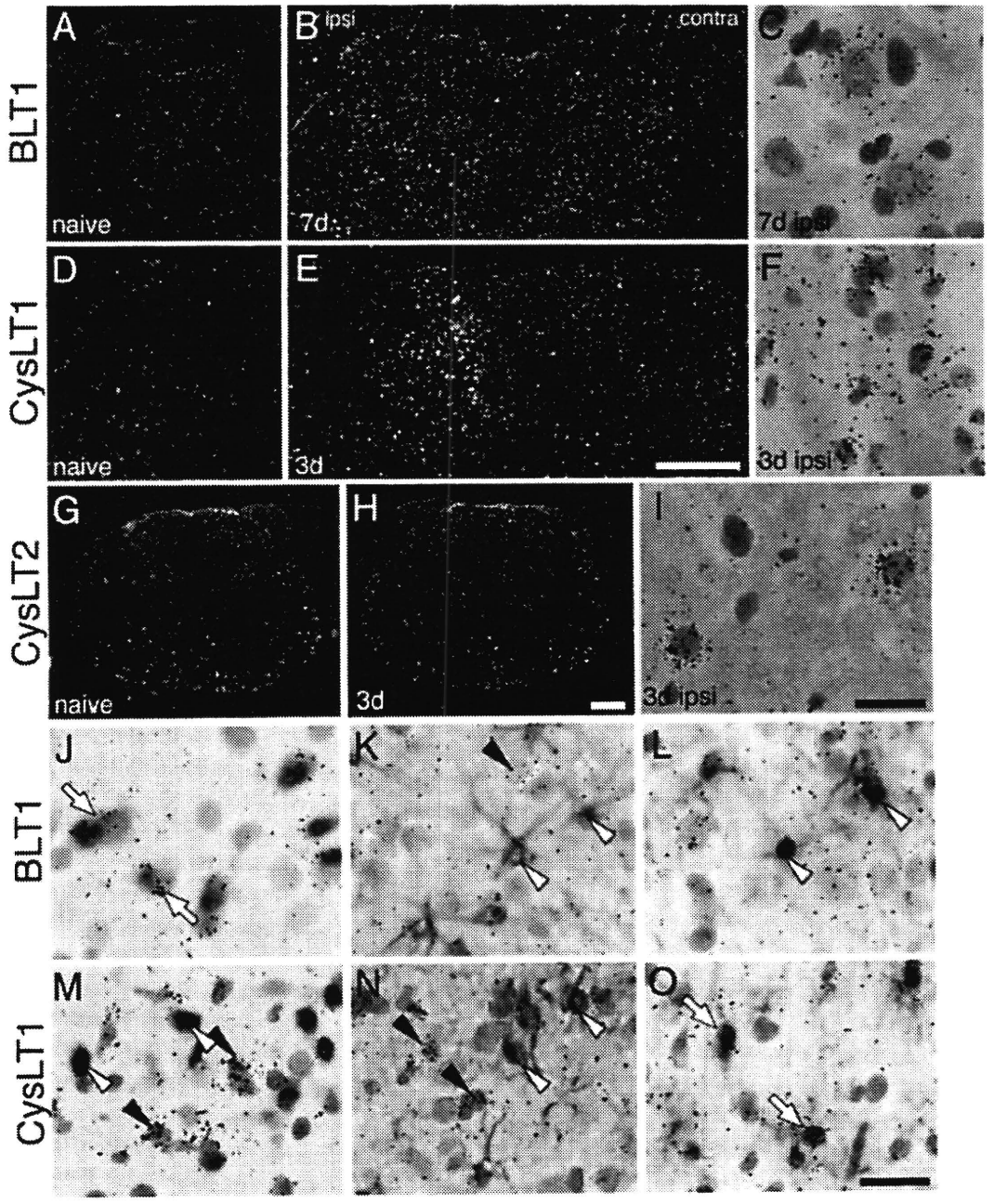

Fig. 6. Peripheral nerve injury enhanced expression of LT receptor mRNAs in ipsilateral spinal neurons and microglia. (A–I) ISHH for LT receptor mRNA expression in the spinal cord; (A–C) BLT1, (D–F) CysLT1, (G–I) CysLT2 in naive rats (A, D, G), 7 days (B) and 3 days after nerve injury (E, H). (C, F, I) Brightfield photographs of the ipsilateral lamina I-II of spinal cord at 7 days (C) or 3 days after nerve injury (F, I). Scale bars: darkfield images; 500 μm, brightfield images; 25 μm. (J–O) Double labeling study of LT receptors. Photographs show combined ISHH for LT receptor mRNAs with NeuN (J, M), GFAP (K, N) and Iba1 (L, O). Photographs of BLT1 (J–L) and CysLT1 (M–O) were taken from the spinal cord of 7 and 3 days after SNI, respectively. Scale bar; 25 μm. Open arrows indicate double-labeled cells. Arrowheads indicate single-labeled cells by ISHH (aggregation of grains), and open arrowheads indicate single immunostained cells (brown staining). [Color figure can be viewed in the online issue, which is available at www.interscience.wiley.com.]

and maintenance of neuropathic pain (Marchand et al., 2005; Milligan and Watkins, 2009; Scholz and Woolf, 2007; Tsuda et al., 2005). Glial activation after nerve injury is thought to trigger the production and release of proinflammatory cytokines and neurotrophins that may augment nociceptive signals in the spinal dorsal horn (Ji and Suter, 2007; Trang et al., 2009). Moreover, a number of substances released from activated glial cells may have an effect on neighboring glial cells, change gene expression, increase the excitability, and enhance the release of proinflammatory mediators, resulting in the enhancement of positive feedback in spinal glial networks (see reviews; Inoue and Tsuda, in press; Ji et al., 2009; Milligan and Watkins, 2009; Scholz and Woolf, 2007). LTs induced and released from activated microglia may have pronociceptive effects onto spinal neurons as well as

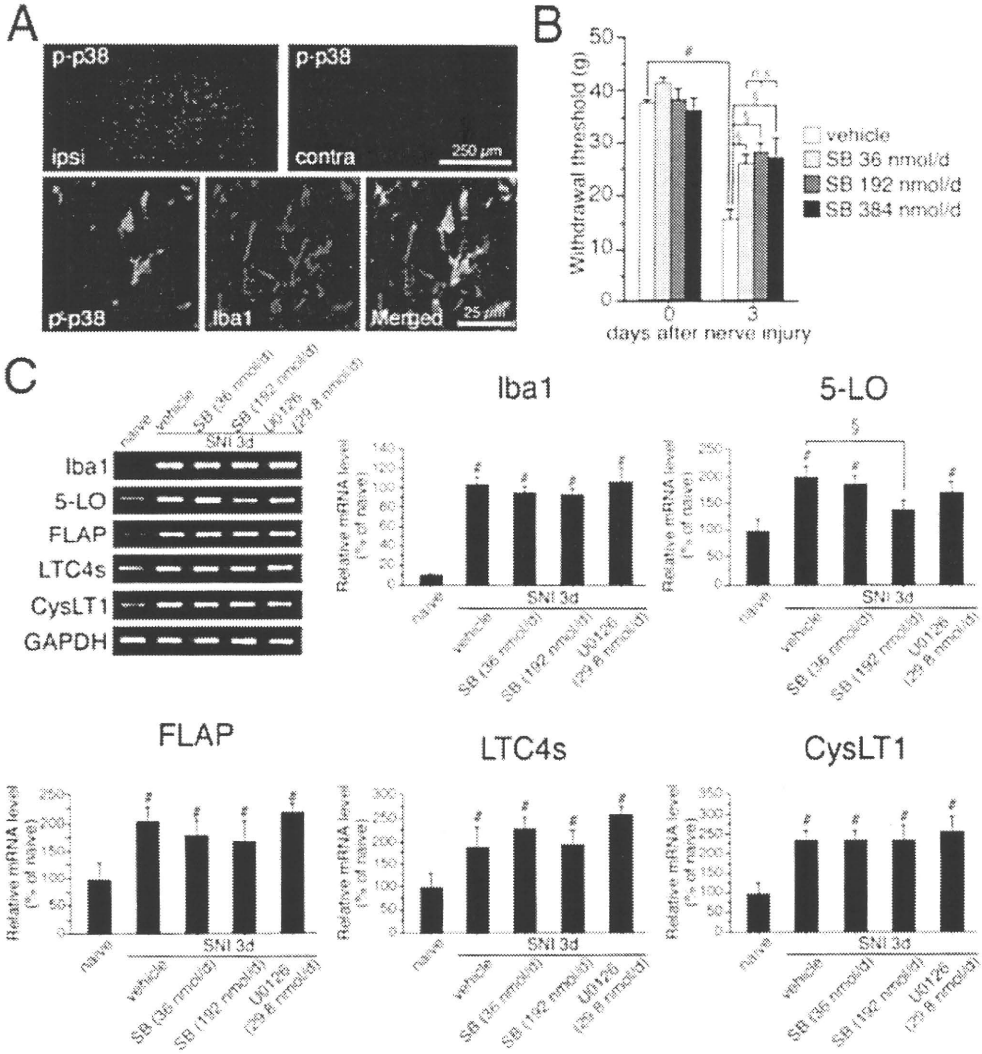

Fig. 7. Pre-treatment of p38 MAPK inhibitor suppressed the expression of 5-LO mRNA induced by SNI in the spinal cord. (**A**) Peripheral nerve injury induced phosphorylation of p38 (p-p38) in the ipsilateral dorsal horn (upper figures). Double staining demonstrated a heavy colocalization of p-p38 (green) with Iba1 (red) in spinal microglia at 3 days after SNI (lower figures). (**B**) Dose responses of the p38 inhibitor on mechanical allodynia induced by SNI surgery. (**C**) Effect of MAPK inhibitors on the induction of LT synthase and receptor mRNA. Gel panels show RT-PCR products from the L4-L5 spinal cord taken from naive, 3 days after SNI administered with vehicle, lower (36 nmol days^{-1}) or higher (196 nmol days^{-1}) concentration of SB203580 and U0126 (29.8 nmol days^{-1}). Graphs show quantification of the relative mRNA levels of LT synthases and the receptors. LT synthase and receptor mRNA levels were normalized against GAPDH ($n = 4$, mean ± SEM, #; $P < 0.05$ compared with naive, §; $P < 0.05$ compared with vehicle). SB indicates SB203580. [Color figure can be viewed in the online issue, which is available at www.interscience.wiley.com.]

within glial networks. Of course, the detailed mechanism how the BLT1 expressed in neurons is activated by binding LTB4 should be explored, but LTs in the spinal cord may be important mediator in the neuropathic pain mechanisms, in addition to other lipid mediators, prostaglandins, or lysophosphatidic acid (Ueda, 2008; Zhao et al., 2000).

In the present study, the effects of LT synthesis on pain behaviors were examined just after the upregulation of several LTs mRNAs were confirmed. Previous studies reported that some lipoxygenase metabolites are involved in hyperalgesia in peripheral inflammation (Jain et al., 2001; Levine et al., 1984; Martin et al., 1988; Trang et al., 2004). In these cases, LTs were released from infiltrated immune cells, such as neutrophils, and may have an effect on nociceptors in peripheral inflamed tissues. LTs have important roles in variety of systemic diseases (Henderson, 1994; Peters-Golden and Henderson, 2007), but few reports have suggested a possible role of LTs on neuropathic pain via intraspinal mechanisms. Findings that the intrathecal injection of 5-LO inhibitors and CysLT1 receptor antagonists significantly suppressed the development of mechanical allodynia after SNI suggest an intraspinal role of LTs in neuropathic pain. Like other molecules synthesized in activated microglia, LTs has positive effects on pain behaviors for limited periods after nerve injury. Because the delayed application of LTs antagonists showed no effects on pain behaviors, we believe that CysLT1 in microglia and BLT1 in neurons are involved in the early phase of neuropathic pain, not in its maintenance.

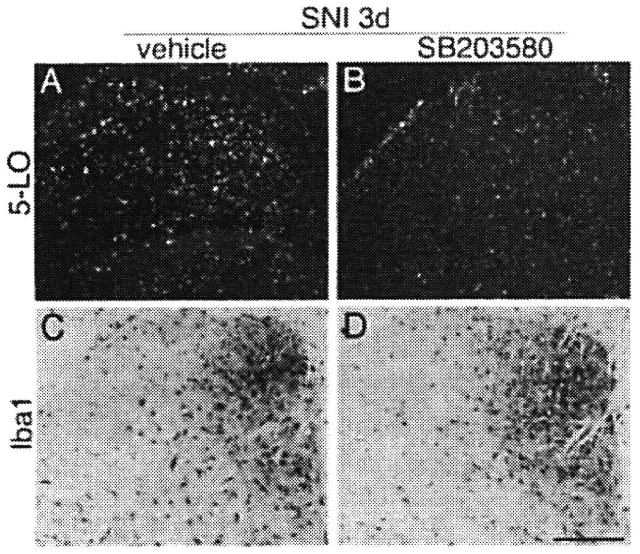

Fig. 8. The p38 MAPK inhibitor reduced the number of 5-LO mRNAs induced by SNI 3d after surgery. (**A**, **B**) Darkfield photographs of ISHH show 5-LO mRNA in the spinal cord of SNI rats treated with vehicle and p38 MAPK inhibitor SB203580 (196 nmol days $^{-1}$). (**C**, **D**) Immunohistochemical photographs show Iba1 in the spinal cord of SNI rats treated with vehicle and SB203580. Scale bars: 250 μm.

MAPK plays a critical role in intracellular signal transduction and consist of ERK1/2, p38 MAPK, and JNK1/2 (Chang and Karin, 2001; Widmann et al., 1999). Emerging evidence indicates that nerve injury results in MAPK activation in spinal glial cells, and MAPK inhibitors diminish injury-induced pain hypersensitivity (Ji and Suter, 2007; Ji et al., 2009; Jin et al., 2003; Katsura et al., 2008; Kobayashi et al., 2008; Scholz and Woolf, 2007; Trang et al., 2009). In the present study, we found that a p38 MAPK inhibitor, SB203580, significantly reduced nerve injury-induced 5-LO mRNA upregulation in spinal microglia, although other enzymes, FLAP, LTC4s, etc. did not change as a result of the treatment with p38 inhibitor. These findings suggest that nerve injury activates the first step of sequential LTs pathway, 5-LO, in spinal microglia via p38 MAPK activation, and thus increase mechanical hypersensitivity.

Based on the findings described in this present study (Fig. 1C), we hypothesize a novel lipid mediator working in the spinal cord during peripheral nerve injury. The LTs synthetic enzymes, such as 5-LO, FLAP, LTA4h, and LTC4s, increased in microglia after SNI injury via the p38 MAPK pathway. At the same time, the LTs receptors, BLT1 and CysLT1, increased in spinal neurons and microglia, respectively. The signaling via LTs and the receptors between microglia and neurons or among microglia may be involved in the development of mechanical allodynia after peripheral nerve injury. Of course, how neurons in the dorsal horn with BLT1 contribute to increased pain behaviors should be examined, and how the signaling in microglial network via LTs affects on nociception is also a next important research question.

ACKNOWLEDGMENTS

The authors thank Dr. D.A. Thomas for correcting the English usage on this manuscript.

REFERENCES

Bisgaard H, Kristensen JK. 1985. Leukotriene B4 produces hyperalgesia in humans. Prostaglandins 30:791–797.
Chang L, Karin M. 2001. Mammalian MAP kinase signalling cascades. Nature 410:37–40.
Chen ZL, Yoshida S, Kato K, Momota Y, Suzuki J, Tanaka T, Ito J, Nishino H, Aimoto S, Kiyama H, Shiosaka S. 1995. Expression and activity-dependent changes of a novel limbic-serine protease gene in the hippocampus. J Neurosci 15:5088–5097.
Decosterd I, Woolf CJ. 2000. Spared nerve injury: An animal model of persistent peripheral neuropathic pain. Pain 87:149–158.
DeLeo JA, Yezierski RP. 2001. The role of neuroinflammation and neuroimmune activation in persistent pain. Pain 90:1–6.
Heise CE, O'Dowd BF, Figueroa DJ, Sawyer N, Nguyen T, Im DS, Stocco R, Bellefeuille JN, Abramovitz M, Cheng R, Williams DL Jr, Zeng Z, Liu Q, Ma L, Clements MK, Coulombe N, Liu Y, Austin CP, George SR, O'Neill GP, Metters KM, Lynch KR, Evans JF. 2000. Characterization of the human cysteinyl leukotriene 2 receptor. J Biol Chem 275:30531–30536.
Henderson WR Jr. 1994. The role of leukotrienes in inflammation. Ann Intern Med 121:684–697.
Inoue K, Tsuda M. Microglia and neuropathic pain. Glia 57:1469–1479.
Inoue M, Rashid MH, Fujita R, Contos JJ, Chun J, Ueda H. 2004. Initiation of neuropathic pain requires lysophosphatidic acid receptor signaling. Nat Med 10:712–718.
Jain NK, Kulkarni SK, Singh A. 2001. Role of cysteinyl leukotrienes in nociceptive and inflammatory conditions in experimental animals. Eur J Pharmacol 423:85–92.
Ji RR, Suter MR. 2007. p38 MAPK, microglial signaling, and neuropathic pain. Mol Pain 3:33.
Ji RR, Gereau RWT, Malcangio M, Strichartz GR. 2009. MAP kinase and pain. Brain Res Rev 60:135–148.
Jin SX, Zhuang ZY, Woolf CJ, Ji RR. 2003. p38 mitogen-activated protein kinase is activated after a spinal nerve ligation in spinal cord microglia and dorsal root ganglion neurons and contributes to the generation of neuropathic pain. J Neurosci 23:4017–4022.
Kalmar B, Greensmith L, Malcangio M, McMahon SB, Csermely P, Burnstock G. 2003. The effect of treatment with BRX-220, a co-inducer of heat shock proteins, on sensory fibers of the rat following peripheral nerve injury. Exp Neurol 184:636–647.
Katsura H, Obata K, Miyoshi K, Kondo T, Yamanaka H, Kobayashi K, Dai Y, Fukuoka T, Sakagami M, Noguchi K. 2008. Transforming growth factor-activated kinase 1 induced in spinal astrocytes contributes to mechanical hypersensitivity after nerve injury. Glia 56:723–733.
Kobayashi K, Fukuoka T, Yamanaka H, Dai Y, Obata K, Tokunaga A, Noguchi K. 2006. Neurons and glial cells differentially express P2Y receptor mRNAs in the rat dorsal root ganglion and spinal cord. J Comp Neurol 498:443–454.
Kobayashi K, Yamanaka H, Fukuoka T, Dai Y, Obata K, Noguchi K. 2008. P2Y12 receptor upregulation in activated microglia is a gateway of p38 signaling and neuropathic pain. J Neurosci 28:2892–2902.
Lever I, Cunningham J, Grist J, Yip PK, Malcangio M. 2003. Release of BDNF and GABA in the dorsal horn of neuropathic rats. Eur J Neurosci 18:1169–1174.
Levine JD, Lau W, Kwiat G, Goetzl EJ. 1984. Leukotriene B4 produces hyperalgesia that is dependent on polymorphonuclear leukocytes. Science 225:743–745.
Lynch KR, O'Neill GP, Liu Q, Im DS, Sawyer N, Metters KM, Coulombe N, Abramovitz M, Figueroa DJ, Zeng Z, Connolly BM, Bai C, Christopher P, Austin CP, Chateauneuf A, Stocco R, Greig GM, Kargman S, Hooks SB, Hosfield E, Williams DL Jr, Ford-Hutchinson AW, Caskey CT, Evans JF. 1999. Characterization of the human cysteinyl leukotriene CysLT1 receptor. Nature 399:789–793.
Ma W, Quirion R. 2008. Does COX2-dependent PGE2 play a role in neuropathic pain? Neurosci Lett 437:165–169.
Marchand F, Perretti M, McMahon SB. 2005. Role of the immune system in chronic pain. Nat Rev Neurosci 6:521–532.
Martin HA, Basbaum AI, Goetzl EJ, Levine JD. 1988. Leukotriene B4 decreases the mechanical and thermal thresholds of C-fiber nociceptors in the hairy skin of the rat. J Neurophysiol 60:438–445.

Milligan ED, Watkins LR. 2009. Pathological and protective roles of glia in chronic pain. Nat Rev Neurosci 10:23–36.
Moriyama T, Higashi T, Togashi K, Iida T, Segi E, Sugimoto Y, Tominaga T, Narumiya S, Tominaga M. 2005. Sensitization of TRPV1 by EP1 and IP reveals peripheral nociceptive mechanism of prostaglandins. Mol Pain 1:3.
O'Rielly DD, Loomis CW. 2006. Increased expression of cyclooxygenase and nitric oxide isoforms, and exaggerated sensitivity to prostaglandin E2, in the rat lumbar spinal cord 3 days after L5-L6 spinal nerve ligation. Anesthesiology 104:328–337.
Peters-Golden M, Henderson WR Jr. 2007. Leukotrienes. N Engl J Med 357:1841–1854.
Scholz J, Woolf CJ. 2002. Can we conquer pain? Nat Neurosci 5 (Suppl):1062–1067.
Scholz J, Woolf CJ. 2007. The neuropathic pain triad: Neurons, immune cells and glia. Nat Neurosci 10:1361–1368.
Trang T, McNaull B, Quirion R, Jhamandas K. 2004. Involvement of spinal lipoxygenase metabolites in hyperalgesia and opioid tolerance. Eur J Pharmacol 491:21–30.
Trang T, Beggs S, Wan X, Salter MW. 2009. P2X4-receptor-mediated synthesis and release of brain-derived neurotrophic factor in microglia is dependent on calcium and p38-mitogen-activated protein kinase activation. J Neurosci 29:3518–3528.
Tsuda M, Inoue K, Salter MW. 2005. Neuropathic pain and spinal microglia: A big problem from molecules in "small" glia. Trends Neurosci 28:101–107.
Tsuda M, Ishii S, Masuda T, Hasegawa S, Nakamura K, Nagata K, Yamashita T, Furue H, Tozaki-Saitoh H, Yoshimura M, Koizumi S, Shimizu T, Inoue K. 2007. Reduced pain behaviors and extracellular signal-related protein kinase activation in primary sensory neurons by peripheral tissue injury in mice lacking platelet-activating factor receptor. J Neurochem 102:1658–1668.
Ueda H. 2008. Peripheral mechanisms of neuropathic pain—Involvement of lysophosphatidic acid receptor-mediated demyelination. Mol Pain 4:11.
Watkins LR, Maier SF. 2003. Glia: A novel drug discovery target for clinical pain. Nat Rev Drug Discov 2:973–985.
Watkins LR, Milligan ED, Maier SF. 2001a. Glial activation: A driving force for pathological pain. Trends Neurosci 24:450–455.
Watkins LR, Milligan ED, Maier SF. 2001b. Spinal cord glia: New players in pain. Pain 93:201–205.
Widmann C, Gibson S, Jarpe MB, Johnson GL. 1999. Mitogen-activated protein kinase: Conservation of a three-kinase module from yeast to human. Physiol Rev 79:143–180.
Woolf CJ, Salter MW. 2000. Neuronal plasticity: Increasing the gain in pain. Science 288:1765–1769.
Yamanaka H, Obata K, Fukuoka T, Dai Y, Kobayashi K, Tokunaga A, Noguchi K. 2004. Tissue plasminogen activator in primary afferents induces dorsal horn excitability and pain response after peripheral nerve injury. Eur J Neurosci 19:93–102.
Yamanaka H, Obata K, Fukuoka T, Dai Y, Kobayashi K, Tokunaga A, Noguchi K. 2005. Induction of plasminogen activator inhibitor-1 and -2 in dorsal root ganglion neurons after peripheral nerve injury. Neuroscience 132:183–191.
Yao Y, Wolverton JE, Zhang Q, Marathe GK, Al-Hassani M, Konger RL, Travers JB. 2009. Ultraviolet B radiation generated platelet-activating factor receptor agonist formation involves EGF-R-mediated reactive oxygen species. J Immunol 182:2842–2848.
Yokomizo T, Izumi T, Chang K, Takuwa Y, Shimizu T. 1997. A G-protein-coupled receptor for leukotriene B4 that mediates chemotaxis. Nature 387:620–624.
Yokomizo T, Kato K, Terawaki K, Izumi T, Shimizu T. 2000. A second leukotriene B(4) receptor, BLT2 A new therapeutic target in inflammation and immunological disorders. J Exp Med 192:421–432.
Zhao Z, Chen SR, Eisenach JC, Busija DW, Pan HL. 2000. Spinal cyclooxygenase-2 is involved in development of allodynia after nerve injury in rats. Neuroscience 97:743–748.
Zhuang ZY, Wen YR, Zhang DR, Borsello T, Bonny C, Strichartz GR, Decosterd I, Ji RR. 2006. A peptide c-Jun N-terminal kinase (JNK) inhibitor blocks mechanical allodynia after spinal nerve ligation: Respective roles of JNK activation in primary sensory neurons and spinal astrocytes for neuropathic pain development and maintenance. J Neurosci 26:3551–3560.

Okubo et al. Molecular Pain 2010, 6:57
http://www.molecularpain.com/content/6/1/57

MOLECULAR PAIN

RESEARCH Open Access

Expression of leukotriene receptors in the rat dorsal root ganglion and the effects on pain behaviors

Masamichi Okubo[1], Hiroki Yamanaka[1], Kimiko Kobayashi[1], Tetsuo Fukuoka[1], Yi Dai[2], Koichi Noguchi[1*]

Abstract

Background: Leukotrienes (LTs) belong to the large family of lipid mediators implicated in various inflammatory conditions such as asthma and rheumatoid arthritis. Four distinct types (BLT1, BLT2, CysLT1 and CysLT2) of G-protein-coupled receptors for LTs have been identified. Several studies have reported that LTs are involved in inflammatory pain, but the mechanism and the expression of LT receptors in the nociceptive pathway are unknown.

Results: We investigated the precise expression of these four types of LT receptors in the adult rat dorsal root ganglion (DRG) using reverse transcription-polymerase reaction (RT-PCR) and radioisotope-labeled *in situ* hybridization histochemistry (ISHH). We detected mRNAs for BLT1 and CysLT2 in the DRG, but not for BLT2 and CysLT1. CysLT2 mRNA was preferentially expressed by small sized DRG neurons (about 36% of total neurons), whereas BLT1 mRNA was expressed by non-neuronal cells. Double labeling analysis of CysLT2 with NF-200, calcitonin gene-related peptide (CGRP), isolectin B4 (IB4), transient receptor potential vanilloid subfamily 1 (TRPV1) and P2X3 receptor revealed that many CysLT2-labeled neurons were localized with unmyelinated and non-peptidergic neurons, and interestingly, CysLT2 mRNA heavily co-localized with TRPV1 and P2X3-positive neurons. Intraplantar injection of LTC4, a CysLT2 receptor agonist, itself did not induce the thermal hyperalgesia, spontaneous pain behaviors or swelling of hind paw. However, pretreatment of LTC4 remarkably enhanced the painful behaviors produced by alpha, beta-methylene adenosine 5'-triphosphate ($\alpha\beta$-me-ATP), a P2X3 receptor agonist.

Conclusions: These data suggests that CysLT2 expressed in DRG neurons may play a role as a modulator of P2X3, and contribute to a potentiation of the neuronal activity following peripheral inflammation.

Background

The leukotrienes (LTs) are a family of biologically active lipid mediators. They are synthesized from arachidonic acid (AA) *via* the 5-lipoxygenase pathway. AA is enzymatically converted to LTB4, LTC4, LTD4 and LTE4 that are known as bioactive LTs. LTC4, LTD4 and LTE4 are collectively termed the cysteinyl leukotrienes (CysLTs). LTs are peripherally produced by activated leukocytes in response to peripheral inflammation, such as asthma and atopic dermatitis [1,2]. Four different types (BLT1, BLT2, CysLT1 and CysLT2) of G-protein-coupled receptor for LT have been cloned [3-6]. LTB4 activates BLT1 and BLT2, and CysLTs activate CysLT1 and CysLT2.

Peripheral inflammation often elicits mechanical and thermal hyperalgesia. The most studied of these lipid mediators are the prostaglandins (PGs) of the cyclooxygenase pathway of AA metabolism [7,8]. Expression of G-protein-coupled receptors of EP for E-type PG is localized in C-fibers, unmyelinated nociceptive fibers, in the dorsal root ganglion (DRG) [8]. Activation of EP signaling plays a role in neuronal sensitization mediating modulation of the transient receptor potential vanilloid subfamily 1 (TRPV1) receptor and P2X3 receptor [9,10].

Intradermal injection of LTB4 has been shown to produce both thermal and mechanical hyperalgesia [11,12].

* Correspondence: noguchi@hyo-med.ac.jp
[1]Department of Anatomy and Neuroscience, Hyogo College of Medicine, 1-1 Mukogawa-cho, Nishinomiya, Hyogo 663-8501, Japan
Full list of author information is available at the end of the article

Jain et al. have reported that LTs are involved in inflammatory pain induced by carrageenan [13]. Furthermore, we demonstrated that an increase in LT synthesis in microglia in the spinal cord induced by peripheral nerve injury contributes to neuropathic pain [14]. However, in the periphery, the mechanism of the nociception induced by LTs is unknown and the precise expression pattern of LT receptors in the DRG has not been clarified. The purpose of this study is to examine the expression of LT receptor mRNAs in the DRG to assess whether LT receptors are expressed in nociceptive neurons. Furthermore, we attempted to determine the nociceptive role of LT receptors in DRG by behavioral analyses.

Results

Expression of LT receptors in the DRG

To examine whether sensory neurons express the LT receptor mRNAs, we performed reverse transcription-polymerase chain reaction (RT-PCR) and *in situ* hybridization histochemistry (ISHH) using adult rat DRG. The mRNAs for BLT1 and CysLT2 mRNAs were expressed in the DRG, but not the BLT2 and CysLT1 mRNAs (Figure 1A). For the ISHH, the BLT1 mRNA was expressed in an extremely limited population of non-neuronal cells (Figure 1B, C). With brightfield imaging of ISHH for the BLT1 mRNA, silver grains were accumulated over the non-neuronal cells whose nuclei were heavily stained with hematoxylin (Figure 1C). In contrast to the BLT1 mRNA, a subpopulation of DRG neurons expressed CysLT2 mRNA (Figure 1D, E). The darkfield photograph displayed distinguishable clusters of silver grains over the tissue with minimal background signals (Figure 1D). The brightfield and high magnification images confirmed the presence of CysLT2 on neuronal cell bodies (Figure 1E). To evaluate objectively the expression of the CysLT2 mRNA in DRG neurons, we measured, calculated, and plotted the signal-to-noise (S/N) ratio and cross-sectional area of each

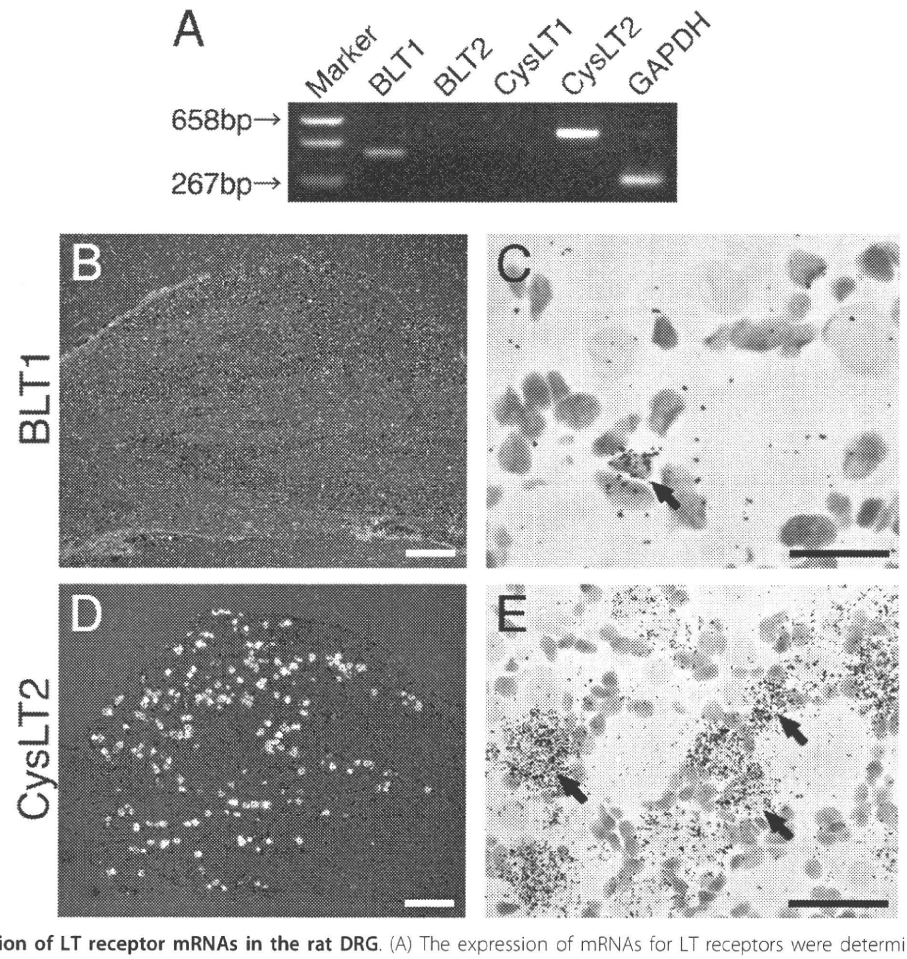

Figure 1 Expression of LT receptor mRNAs in the rat DRG. (A) The expression of mRNAs for LT receptors were determined by the RT-PCR technique. Gel panel shows PCR products from the L4, 5 DRGs taken from naive rats. (B, D) Low-magnification darkfield images of ISHH show BLT1 and CysLT2 mRNAs of naive rats, respectively. (C, E) Higher-magnification brightfield images of the left-hand images. Arrows indicate positively labeled cells by ISHH. Scale bars: B, D; 500 μm, E; 25 μm, C; 12.5 μm.

neuron (Figure 2). Based on this scattergram, neuronal profiles with a grain density of 20-fold the background level or higher (S/N ratio > 20) were considered positively labeled for this mRNA. With this criterion, 35.8 ± 3.3% of profiles were positively labeled for CysLT2 mRNA of the total DRG neurons (Table 1). The scattergram revealed that CysLT2 mRNA was expressed more intensely by the neurons with cell profiles less than 600 μm^2 compared with the medium or large-size neurons. The size distribution of the positively labeled profiles for CysLT2 mRNA is shown in Table 1. The CysLT2 mRNA was expressed in a limited population of small (< 600 μm^2) and medium-size (600-1200 μm^2) neurons, whereas large-size (> 1200 μm^2) neurons were not labeled for this mRNA (Table 1). The neuronal size definition was described previously [15].

Characterization of CysLT2-labeled neurons

To characterize the expression of CysLT2 mRNA in DRG neurons, we used double labeling ISHH with immunohistochemistry (IHC) for NF-200, a maker of myelinated A-fiber neurons. We found NF-200-immunoreactive neurons in 36.3 ± 1.5% of the total neurons (Table 2). No specific staining was observed in the absence of the primary antibody (data not shown). The results of double labeling analysis of CysLT2 mRNA with NF-200 showed that 9.6 ± 3.4% of the CysLT2 mRNA-positive profiles expressed NF-200, conversely, 8.0 ± 2.3% of NF-200-profiles expressed CysLT2 mRNA (Figure 3A; Table 2). The CysLT2 mRNA was expressed in 44.0% of NF-200 negative profiles, which were considered unmyelinated neurons (C-fiber). We tested the co-expression of CysLT2 mRNA with CGRP and IB4 in order to identify the peptide-dependent neuronal subpopulations [16], using

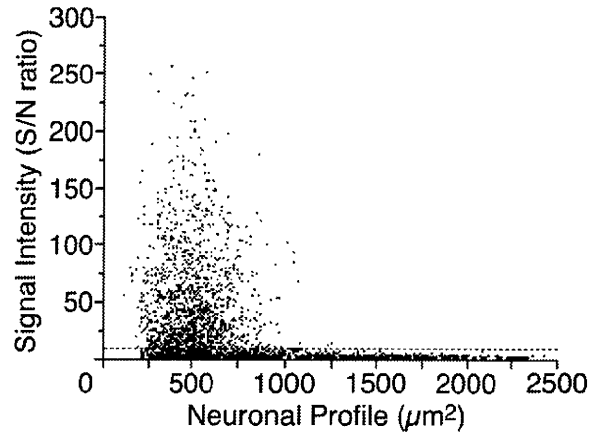

Figure 2 Scatterplot diagram of the DRG neurons expressed mRNA for CysLT2. Individual cell profiles are plotted according to the cross-sectional area and signal intensity (n = 4, 2819 cells). The dashed line indicates the borderline between the negatively and positively labeled neurons (S/N ratio = 20).

Table 1 Distribution of CysLT2 mRNA Expression in the DRG

	Small (< 600 μm^2)	Medium (600-1200 μm^2)	Large (> 1200 μm^2)
CysLT2	76.5 ± 6.5	23.5 ± 6.5	0.0 ± 0.0

Percentages of CysLT2 mRNA-expressing cells in total positive cells. Mean ± SEM (n = 4).

double labeling of ISHH with IHC. We observed CGRP-immunoreactive and IB4-binding neurons in 39.0 ± 3.1% and 37.5 ± 2.9% of the total neuronal profiles, respectively (Table 2). The results of the double labeling analysis of CysLT2 mRNA with CGRP and IB4 showed that 27.5% of the CysLT2 mRNA-positive profiles expressed CGRP; conversely, 25.6% of CGRP-profiles expressed CysLT2 mRNA (Figure 3B, Table 2), and 85.6% of the CysLT2 mRNA-positive profiles expressed IB4, conversely, 82.0% of IB4-profiles expressed CysLT2 mRNA (Figure 3C, Table 2). These results indicated that CysLT2 mRNA was expressed in non-peptidergic neurons rather than peptidergic neurons.

Next, to examine whether CysLT2 mRNA was co-expressed with TRPV1 and P2X3 that are considered as pivotal nociceptors in primary afferent fibers, we tested the percentage of colocalization of CysLT2 mRNA with TRPV1 and P2X3. We observed TRPV1 and P2X3-ir neurons in 36.7 ± 1.5% and 34.0 ± 1.9% of the total neuronal profiles, respectively (Table 2). Further, 71.2% of the CysLT2 mRNA-positive profiles expressed TRPV1; conversely, 69.6% TRPV1- positive profiles expressed CysLT2 mRNA (Figure 3D; Table 2) and 80.7% of the CysLT2 mRNA-positive profiles expressed P2X3; conversely, 88.8% P2X3- positive profiles expressed CysLT2 mRNA (Figure 3E; Table 3).

Effect of LTC4, a CysLT2 receptor agonist, on pain-related behaviors

Leukotrienes are known as proinflammatory lipid mediators, and CysLT2 was co-localized with TRPV1, a heat

Table 2 Percentages of Colocalization of CysLT2 mRNA with NF-200, CGRP, IB4, TRPV1 and P2X3 Immunoreactive Neurons in DRG

y	*x/y*	*y/x*
NF-200 (36.3%)	8.0 ± 2.3	9.6 ± 3.4
CGRP (39.0%)	25.6 ± 3.0	27.5 ± 3.9
IB4 (37.5%)	82.0 ± 4.6	85.6 ± 1.5
TRPV1 (36.7%)	69.6 ± 4.6	71.2 ± 1.8
P2X3 (34.0%)	88.8 ± 2.2	80.7 ± 3.7

x/y means the percentage of CysLT2 (x) mRNA-expressing cells in y immunoreactive cells. (number); means percentage of the neurons expressing the corresponding immunoreactivity in total DRG neurons. Mean ± SEM (n = 4).

sensor, in DRG neurons. We examined whether LTC4, a CysLT2 receptor agonist, leads to thermal hyperalgesia (Figure 4A). We tested heat sensitivity of the hind paw after intraplantar injection of LTC4 (8 fmol, 0.8 pmol and 80 pmol). None of doses affected on heat sensitivity at 10, 30 and 60 min after LTC4 injection (Figure 4A). LTC4 alone (0.8 pmol) did not contribute to the nocifensive behaviors (pain-like behaviors) and swelling of the hind paw (data not shown).

Next, because CysLT2-positive cells heavily co-localized with P2X3, we examined whether intraplantar injection of LTC4 can enhance the nocifensive behaviors induced by alpha, beta-methylene adenosine 5'-triphosphate (αβ-me-ATP), a P2X3 receptor agonist. In normal rats, αβ-me-ATP (100 μmol) consistently induced periods of intermittent hind paw-lifting behavior, which mostly began within 30-40 s after the injection and continued for the first 4 min [17]. Intraplantar injection of LTC4 at 0.8 pmol before the αβ-me-ATP injection induced a remarkable increase of paw-lifting behaviors (Figure 4B). The increase of duration of paw lifting was significantly larger than that after the injection of PBS plus αβ-me-ATP (Figure 4B). Lower and higher doses of LTC4 (< 80 fmol and 8 pmol <) did not show the alteration of nocifensive behaviors by αβ-me-ATP injection (Figure 4B). Potentiation of nocifensive behaviors induced by LTC4 showed a bell-shaped concentration-effect curve, with no significant effect at lower and higher amounts.

Table 3 Sequence Location of Primers Used in This Study

		Primer	
Gene	**GenBank Accession no.**	**Forward**	**Reverse**
BLT1	AB025230	1812-1831	2231-2212
BLT2	AB052660	488-507	939-920
CysLT1	AB052685	234-253	698-679
CysLT2	AB052661	105-124	670-651
GAPDH	M17701	80-99	350-331

Pretreatment with the LTC4 increased αβ-me-ATP-induced Fos expression

A single injection of αβ-me-ATP (100 nmol) induced Fos expression in a small number of spinal neurons (Figure 4C). The labeled neurons were in the superficial dorsal horn but were relatively distributed throughout the spinal cord laminae. The injection of αβ-me-ATP (100 nmol) into the hind paw of the LTC4 (0.8 pmol)-pretreated rats induced elevated Fos expression in spinal neurons (Figure 4D). The Fos-labeled cells were prominently observed in the medial half of the superficial laminae of the spinal dorsal horn. The number of Fos-labeled cells in laminae I-II induced by the injection of αβ-me-ATP (100 nmol) in rats pretreated LTC4 (0.8

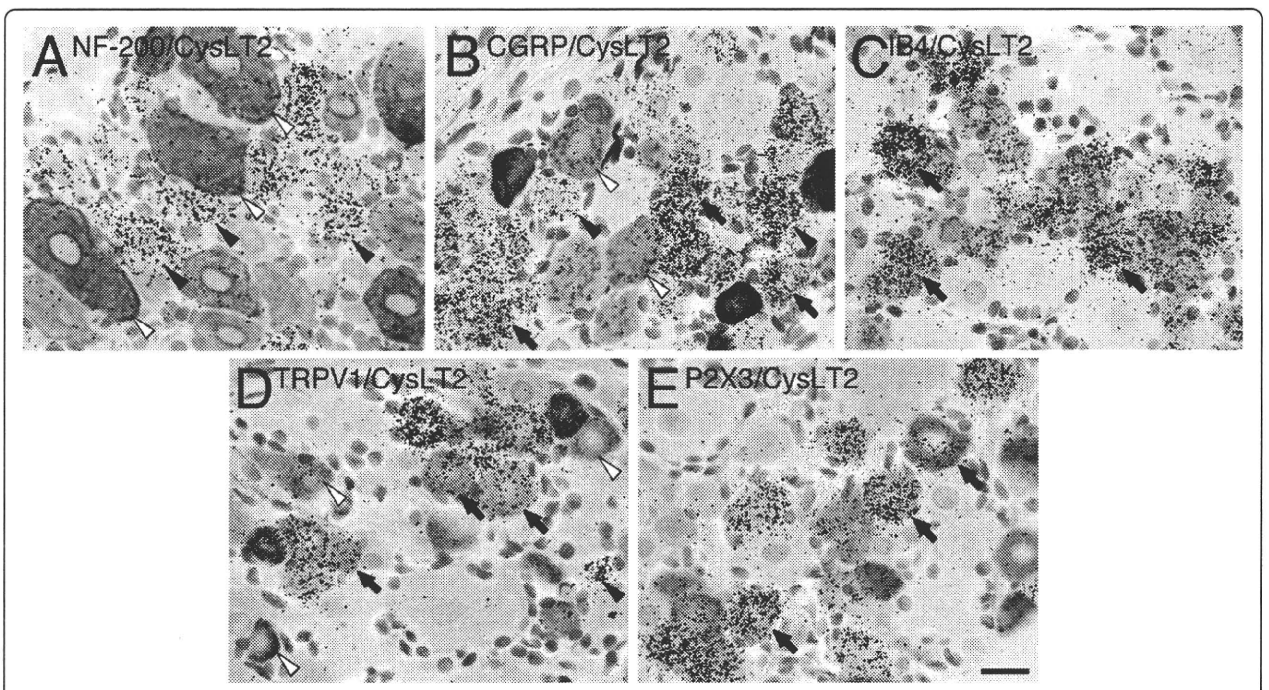

Figure 3 Distribution of CysLT2 mRNA in histochemically identified neuronal subpopulations in the rat DRG. Brightfield images of combined immunohistochemistry for (A) NF-200, (B) CGRP, (C) IB4, (D) TRPV1, (E) P2X3 with ISHH for CysLT2 mRNA. Arrows indicate examples of double-labeled cells. Solid arrowheads indicate positively labeled cells by ISHH and open arrowheads indicate examples of immunoreactive cells. Scale bars; 25 μm.

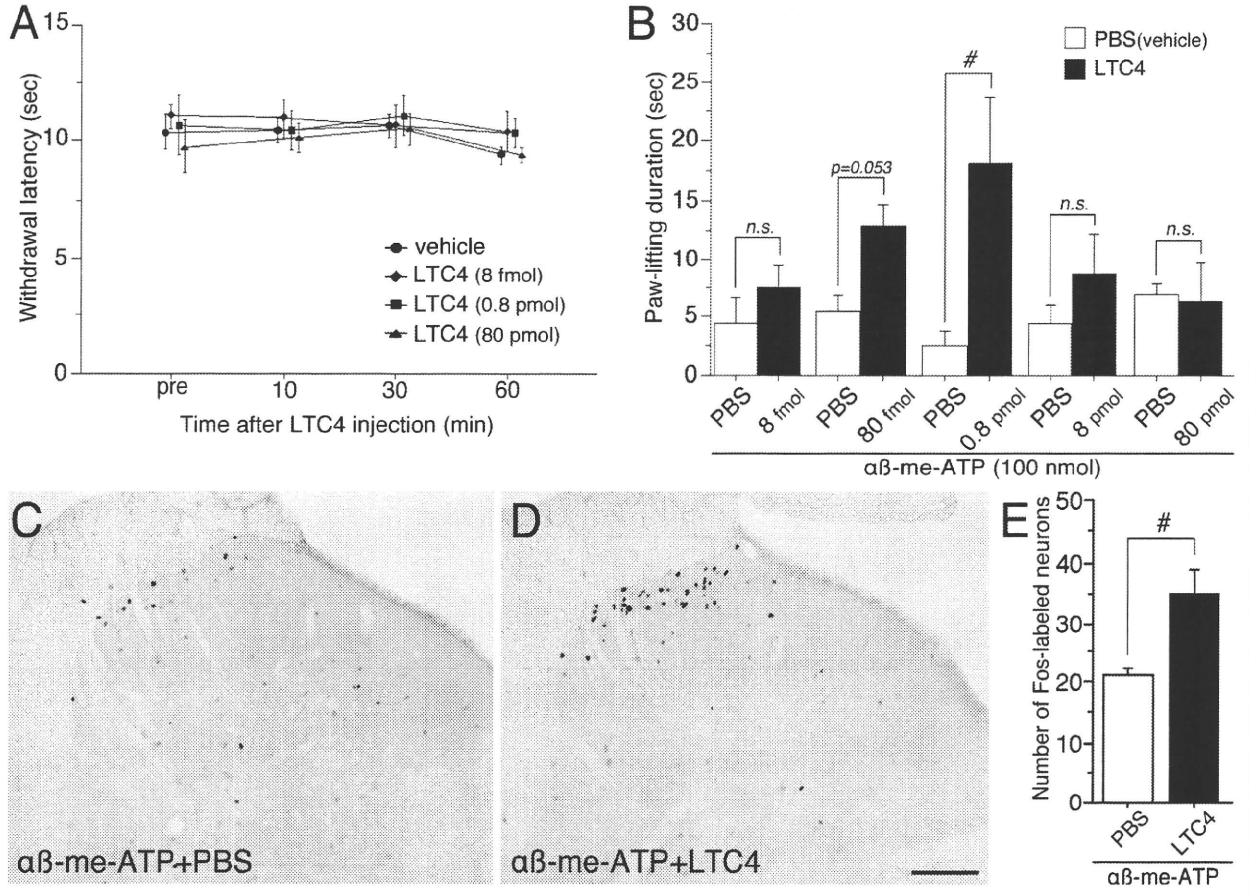

Figure 4 Effect of LTC4, a CysLT2 receptor agonist, on αβ-me-ATP induced pain behaviors and Fos expression. (A) Thermal sensitivity was evaluated by measuring withdrawal latency (sec) at pre (pretreatment), 10, 30 and 60 min after intraplantar injection of LTC4 using a plantar test. (B) The nocifensive behaviors induced by αβ-me-ATP (100 nmol) were evaluated by measuring paw-lifting duration (sec). LTC4 was given at several doses of 8 fmol - 80 pmol/paw, and the ensuing hind paw-lifting duration over the following 4 min was measured. #p < 0.05 compared with vehicle treated group. n = 4-6 for each group. (C, D) Fos protein immunoreactivity in the L5 spinal cord induced by αβ-me-ATP (100 nmol) alone (C) and LTC4 (0.8 pmol) followed by αβ-me-ATP intraplantar injection (D). (E) Number of Fos-labeled neurons in spinal laminae I-II shown in C and D. #p < 0.05 compared with vehicle treated group. n = 3 for each group. Scale bar: 100 μm.

pmol) was significantly larger (almost 1.5 times) than those pretreated with PBS (Figure 4E).

Discussion

LTs are lipid mediators with a proinflammatory profile and have been implicated in the pathogenesis of several types of inflammation [1]. For example, the blood and synovial fluids of patients with rheumatoid arthritis contain higher levels of LTB4 than people without rheumatoid arthritis [18]. LTB4 is known as a potent neutrophil chemotactic agent. It is considered that the neutrophils that are infiltrated by rheumatoid arthritis produce LTB4 in synovial fluids and induce the inflammatory condition. Several studies have demonstrated that LTs are involved in inflammatory pain [11-13]. It is well known that nerve growth factor (NGF) is up-regulated in inflammatory tissue and sensitizes nociceptors [19] leading to thermal hyperalgesia [20]. It has reported that NGF increased LTB4 in the rat paw skin and these results suggested the participation of LTB4 in NGF-induced local thermal hyperalgesia [21]. Furthermore, Trang et al. have reported that intrathecal administration of LTB4 leads to thermal hyperalgesia, and a BLT1 receptor antagonist suppresses this hyperalgesia [22]. These previous reports indicate that LTs in peripheral tissues may have an effect on primary afferents.

In the present study, we demonstrated the expression of LT receptors, BLT1, BLT2, CysLT1, and CysLT2, in the adult rat DRG. We could not detect BLT2 and CysLT1 mRNAs in the DRG. We found the BLT1 mRNA expression in non-neuronal cells, but Andoh et al. reported expression of BLT1 in mouse DRG neurons [23]. This discrepancy may be due to the difference of the species (rat versus mouse) or the methods (ISHH

versus IHC). In contrast to the expression of BLT1 mRNA, CysLT2 mRNA was expressed in DRG neurons. CysLT2 was cloned in 2000 [5], however, there has been limited information of its tissue distribution in nervous system, such as in the astrocyte in brain [24]. CysLT2 is involved in apoptosis induced by oxygen-glucose deprivation *in vitro* [24], but its functional role remains largely unknown. We precisely quantified CysLT2 mRNA in the adult rat DRG showing that about 40% of DRG neurons expressed CysLT2 mRNA (S/N > 20) and small sized DRG neurons preferentially expressed CysLT2. Double-labeling analysis with NF-200 and CysLT2 showed that most CysLT2-labeled cells did not express NF-200. Moreover, a lot of CysLT2-positive profiles exclusively co-localized with IB4-binding, a quarter of CGRP-positive neurons expressed CysLT2 mRNA. These results indicate that CysLT2 was mainly expressed in unmyelinated and non-peptidergic neurons.

Interestingly, CysLT2 mRNA expressing neurons were heavily co-localized with TRPV1- or P2X3-positive neurons. TRPV1, one of the TRPV family, has been cloned and is a thermosensitive channel with a threshold of 42 degrees Celsius [25]. TRPV1 is expressed in small sized neurons [26] and is modulated by various G-protein coupled receptors, such as EP4 [8], protease-activated receptor 2 [27] and neurokinin-1 receptor [28]*via* the protein kinase C (PKC) pathway. 12-(S)-HPETE, a product of 12-lipoxygenase, potentiates the TRPV1 current in HEK cells [29]. Thompson et al. have reported that the signaling pathway for CysLT2 is involved in the activation of PKC pathway *via* Gq-proteins [30]. Because it is possible that CysLT2 can sensitize TRPV1 in primary sensory neurons, we examined whether intraplantar injection of LTC4 leads to thermal hyperalgesia. All doses of LTC4 (8 fmol, 0.8 pmol and 80 pmol) did not affect on heat sensitivity at 10, 30 and 60 min after the injection in normal rats. The data indicate LTC4 does not have a role on thermal hyperalgesia in a normal condition. However, a further study is required to know the role of LTC4 on thermal sensitivity in tissue inflammation.

P2X3 is a ligand-gated ion channel for ATP, and belongs to P2X family. P2X3 is of particular interest in the context of pain pathways, because it is selectively expressed at high levels by nociceptors [31], and electrophysiological studies suggest that the P2X receptors in sensory neurons may play an important role in the generation and/or modulation of the pain signaling from the periphery to the spinal cord [32]. Furthermore, we previously reported that P2X3 in peripheral afferents plays a role in the induction of the hypersensitivity to mechanical stimulation observed during peripheral inflammation [33] and many P2X3s are co-expressed with protease-activated receptor 2 in the rat dorsal root ganglion neurons. Nocifensive behaviors induced by αβ-me-ATP injection to the hind paw were significantly augmented after the application of protease-activated receptor 2 agonists [17]. Fos expression induced by the αβ-me-ATP injection in dorsal horn neurons was also increased after the pre-application of protease-activated receptor 2 agonists [34]. These previous studies led us to behavioral experiments to study whether the LTC4 have a role in potentiation of pain sensation induced by αβ-me-ATP. Intraplantar injection of LTC4 before the αβ-me-ATP injection induced a significant increase of paw-lifting behaviors and Fos expression in the spinal dorsal horn. Based on the finding described in the present study, we concluded that CysLT2, the receptor of LTC4, located in the primary afferent, might modulate the activation of P2X3 by the injection of αβ-me-ATP.

Conclusions

We found that the CysLT2 is preferentially expressed by small-sized, non-peptidergic and nociceptive neurons expressing TRPV1 or P2X3 in the DRG, and contribute to the potentiation of pain behaviors induced by αβ-me-ATP. Our current observations in the context of previous findings may indicate a novel functional role of CysLT2 in the peripheral nervous system.

Methods

Experimental animals

Male Sprague-Dawley rats weighing 200-250 g were used as subjects. All animal experimental procedures were approved by the Hyogo College of Medicine Committee on Animal Research and were performed in accordance with the National Institutes of Health guidelines on animal care. Rats were used for the behavioral analyses. A few minutes after unilateral intraplantar injection of leukotriene C4 (LTC4, Cayman chemical, Ann Arbor, MI) [5S-hydroxy-6R-(S-glutathionyl)-7E,9E,11Z,14Z-eicosatetraenoic acid] [0.8 pmol-8 nmol in 50 μl of phosphate-buffered saline (PBS)], an agonist of CysLT2 receptor, the rats received intradermal injection of αβ-me-ATP (100 nmol, Sigma, St Louis, Missouri, USA) in 50 μl PBS to the plantar surface of the left hind paw. The rats were placed in a wire mesh cage immediately after the injection, and the duration of hind paw lifting during the first 4 min were measured [17,35]. For measurement of thermal hyperalgesia, the withdrawal latency (sec) of hind paw was measured from 10 to 60 min after intraplantar injection of LTC4. Thermal hyperalgesia was assessed with a plantar test (7370, Ugo Basile, Comerio, Italy). The detailed method of thermal sensitivity measurement in rat hind paw was described previously [36].

Reverse transcription-polymerase chain reaction (RT-PCR) and *in situ* hybridization histochemistry (ISHH)

The rats were killed by decapitation under deep ether anesthesia. L4 and L5 DRGs were removed and rapidly frozen with powdered dry ice and stored at 80°C until use. Extraction of total RNA was done by the single step extraction method using ISOGEN (Nippon Gene, Tokyo, Japan) that was described in a previous paper [37]. The forward and reverse primers specific for rat BLT1, BLT2, CysLT1, CysLT2 and GAPDH were designed as shown in Table 3. Amplification cycle were 33 for each cDNA. The amplified cDNA was cloned into p-GEM T-easy (Promega, MI, USA) and sequenced. These clones were used to generate the cRNA probes for ISHH.

For ISHH, the rats were killed by decapitation under deep ether anesthesia. The bilateral L4 and L5 DRGs were dissected out, rapidly frozen in powdered dry ice, and cut on a cryostat at 5 μm thickness. The protocol for ISHH was base on a publish method [38]. Using the enzyme-digested cloned, α^{35}S UTP-labeled antisense and sense cRNA probe were synthesized. Theα^{35}S-labeled probes in hybridization buffer were placed on the section, and then incubated at 55°C overnight. Sections were then washed and treated with 1 μg/ml RNase A. Subsequently, sections were dehydrated and air-dried. After the hybridization reaction, the slides were coated with NTB emulsion (Kodak, Rochester, NY, USA) and exposed for 3-4 weeks. Once developed in D-19 (Kodak), the sections were stained with hematoxylin-eosin and coverslipped.

Double labeling analysis of ISHH with immunohistochemistry (IHC)

For double labeling of ISHH with IHC, the rats were deeply anesthetized with sodium pentobarbital (70-80 mg / kg body weight, i.p.) and perfused transcardially with 100 ml of 1% paraformaldehyde in 0.1 M phosphate buffer, pH 7.4, followed by 500 ml of 4% paraformaldehyde in 0.1 M phosphate buffer. The L4 and L5 DRGs were dissected out and post-fixed in the same fixative for 4 h at 4°C, followed by immersion in 30% sucrose in 0.1 M phosphate buffer at 4°C overnight. The tissue was frozen in powdered dry ice and cut on a cryostat at 5 μm thickness. The sections were processed for IHC using the ABC method [39]. Following antibodies and binding protein were used: Mouse anti-NF200 monoclonal antiserum (1:40000, Sigma, St. Louis, MO, USA), rabbit anti-CGRP (1:10000, Amersham, Buckinghamshire, UK), isolectin B4 from *Griffonia simplicifolia* (IB4, 1:200, Sigma, St. Louis, MO, USA), rabbit anti-TRPV1 (1:100, Oncogene, Cambridge, MA, USA) and rabbit ant-P2X3 (1:500, Oncogene, Cambridge, MA, USA). The sections were washed in TBS and then incubated in biotinylated anti-rabbit or anti-mouse IgG (1:400; Vector Laboratories, Burlingame, CA, USA) in Tris buffer saline (TBS; Tris-HCl 0.1 M, NaCl 0.15 M) containing 5% serum for 2 h at 4°C, followed by incubation in avidin-biotin-peroxidase complex (Elite ABC kit; Vector, CA, USA) for 1 h at room temperature. The horseradish peroxidase reaction was developed in TBS, pH 7.4, containing 0.05% 3,39-diaminobenzidine tetrahydrochloride (Wako, Tokyo, Japan) and 0.01% hydrogen peroxidase. Sections were then washed in TBS and used for ISHH.

Immunohistochemistry for Fos expression

For Fos protein immunohistochemistry, rats were divided into two experimental groups; group 1: rats received injection of αβ-me-ATP and PBS, and were perfused 2 h after the injection; group 2: rats received injection of αβ-me-ATP and LTC4 (80 pmol) and were perfused 2 h after the injection. After appropriate survival times, the rats were deeply anesthetized and perfused transcardially with 4% paraformaldehyde described in double labeling method. L4/L5 segments of the spinal cord were removed for immunohistochemistry as described previously [40]. Rabbit primary antibody for Fos (1:20000; Ab-5; Oncogene) was used. The number of Fos-labeled neurons in laminas I-II was counted in randomly selected sections (ten out of 18-28 sections per rat). A labeled nucleus was judged as positively labeled only when a structure of appropriate size and shape indicated a clear increase in immunoreactivity above the background, but without considering intensity of the staining.

Quantitative analysis

Measurements of the density of silver grains over randomly selected tissue profiles were performed using a computerized image analysis system (NIH Image, version 1.61), where only neuronal profiles that contained nuclei were used for quantification. At a magnification of 200× and with bright-field illumination, upper and lower thresholds of gray level density were set such that only silver grains were accurately discriminated from the background in the outlined cell or tissue profile and read by the computer pixel-by-pixel. Subsequently, the area of discriminated pixels was measured and divided by the area of the outlined profile, giving a grain density for each cell or tissue profile. To reduce the risk of biased sampling of the data because of varying emulsion thickness, we used a signal-to-noise (S/N) ratio for each cell in each tissue. The S/N ratio of an individual neuron and its cross-sectioned area, which was computed from the outlined profile, was plotted. Based on this scatter gram, neurons with a grain density of ten-fold the background level or higher (20 < S/N ratio) were

considered positively labeled for CysLT2 mRNA. Because a stereological approach was not used in this study, quantification of the data may represent a biased estimate of the actual numbers of neurons. At least 500 neurons from the L4/5 DRG of each rat were measured. The number of positively labeled DRG neurons was divided by the number of neuronal profiles counted in each DRG. For IHC, only the signals that were clearly discriminative immunoreactive profiles were considered as the positive expressions.

Acknowledgements

This study was supported in part by Grants-in-Aid for Scientific Research and Grant for Pain Research Group in Hyogo College of Medicine, from the Japanese Ministry of Education, Science and Culture. We gratefully thank Dr. D.A. Thomas the correcting the English usage on this manuscript.

Author details

[1]Department of Anatomy and Neuroscience, Hyogo College of Medicine, 1-1 Mukogawa-cho, Nishinomiya, Hyogo 663-8501, Japan. [2]Department of Pharmacy, School of Pharmacy, Hyogo University of Health Sciences. Kobe, Hyogo 650-8530, Japan.

Authors' contributions

MO with KK and HY designed and performed all of experiments, analyzed data and drafted the paper. HY, KK, TF, YD and KN supervised the project and edited the manuscript. All authors contributed to data interpretation, have read and approved the final manuscript.

Competing interests

The authors declare that they have no competing interests.

Received: 21 June 2010 Accepted: 17 September 2010
Published: 17 September 2010

References

1. Sala A, Folco G: **Neutrophils, endothelial cells, and cysteinyl leukotrienes: a new approach to neutrophil-dependent inflammation?** *Biochem Biophys Res Commun* 2001, **283**:1003-1006.
2. Henderson WR Jr: **The role of leukotrienes in inflammation.** *Ann Intern Med* 1994, **121**:684-697.
3. Yokomizo T, Izumi T, Chang K, Takuwa Y, Shimizu T: **A G-protein-coupled receptor for leukotriene B4 that mediates chemotaxis.** *Nature* 1997, **387**:620-624.
4. Yokomizo T, Kato K, Terawaki K, Izumi T, Shimizu T: **A second leukotriene B (4) receptor, BLT2. A new therapeutic target in inflammation and immunological disorders.** *J Exp Med* 2000, **192**:421-432.
5. Heise CE, O'Dowd BF, Figueroa DJ, Sawyer N, Nguyen T, Im DS, Stocco R, Bellefeuille JN, Abramovitz M, Cheng R, *et al*: **Characterization of the human cysteinyl leukotriene 2 receptor.** *J Biol Chem* 2000, **275**:30531-30536.
6. Lynch KR, O'Neill GP, Liu Q, Im DS, Sawyer N, Metters KM, Coulombe N, Abramovitz M, Figueroa DJ, Zeng Z, *et al*: **Characterization of the human cysteinyl leukotriene CysLT1 receptor.** *Nature* 1999, **399**:789-793.
7. Juan H: **Prostaglandins as modulators of pain.** *Gen Pharmacol* 1978, **9**:403-409.
8. Lin CR, Amaya F, Barrett L, Wang H, Takada J, Samad TA, Woolf CJ: **Prostaglandin E2 receptor EP4 contributes to inflammatory pain hypersensitivity.** *J Pharmacol Exp Ther* 2006, **319**:1096-1103.
9. Moriyama T, Higashi T, Togashi K, Iida T, Segi E, Sugimoto Y, Tominaga T, Narumiya S, Tominaga M: **Sensitization of TRPV1 by EP1 and IP reveals peripheral nociceptive mechanism of prostaglandins.** *Mol Pain* 2005, **1**:3.
10. Wang C, Li GW, Huang LY: **Prostaglandin E2 potentiation of P2X3 receptor mediated currents in dorsal root ganglion neurons.** *Mol Pain* 2007, **3**:22.
11. Bisgaard H, Kristensen JK: **Leukotriene B4 produces hyperalgesia in humans.** *Prostaglandins* 1985, **30**:791-797.
12. Martin HA, Basbaum AI, Goetzl EJ, Levine JD: **Leukotriene B4 decreases the mechanical and thermal thresholds of C-fiber nociceptors in the hairy skin of the rat.** *J Neurophysiol* 1988, **60**:438-445.
13. Jain NK, Kulkarni SK, Singh A: **Role of cysteinyl leukotrienes in nociceptive and inflammatory conditions in experimental animals.** *Eur J Pharmacol* 2001, **423**:85-92.
14. Okubo M, Yamanaka H, Kobayashi K, Noguchi K: **Leukotriene synthases and the receptors induced by peripheral nerve injury in the spinal cord contribute to the generation of neuropathic pain.** *Glia* 2009, **58**:599-610.
15. Kobayashi K, Fukuoka T, Obata K, Yamanaka H, Dai Y, Tokunaga A, Noguchi K: **Distinct expression of TRPM8, TRPA1, and TRPV1 mRNAs in rat primary afferent neurons with adelta/c-fibers and colocalization with trk receptors.** *J Comp Neurol* 2005, **493**:596-606.
16. Snider WD, McMahon SB: **Tackling pain at the source: new ideas about nociceptors.** *Neuron* 1998, **20**:629-632.
17. Zhu WJ, Dai Y, Fukuoka T, Yamanaka H, Kobayashi K, Obata K, Wang S, Noguchi K: **Agonist of proteinase-activated receptor 2 increases painful behavior produced by alpha, beta-methylene adenosine 5'-triphosphate.** *Neuroreport* 2006, **17**:1257-1261.
18. Davidson EM, Rae SA, Smith MJ: **Leukotriene B4, a mediator of inflammation present in synovial fluid in rheumatoid arthritis.** *Ann Rheum Dis* 1983, **42**:677-679.
19. Nicol GD, Vasko MR: **Unraveling the story of NGF-mediated sensitization of nociceptive sensory neurons: ON or OFF the Trks?** *Mol Interv* 2007, **7**:26-41.
20. Ji RR, Samad TA, Jin SX, Schmoll R, Woolf CJ: **p38 MAPK activation by NGF in primary sensory neurons after inflammation increases TRPV1 levels and maintains heat hyperalgesia.** *Neuron* 2002, **36**:57-68.
21. Amann R, Schuligoi R, Lanz I, Peskar BA: **Effect of a 5-lipoxygenase inhibitor on nerve growth factor-induced thermal hyperalgesia in the rat.** *Eur J Pharmacol* 1996, **306**:89-91.
22. Trang T, McNaull B, Quirion R, Jhamandas K: **Involvement of spinal lipoxygenase metabolites in hyperalgesia and opioid tolerance.** *Eur J Pharmacol* 2004, **491**:21-30.
23. Andoh T, Kuraishi Y: **Expression of BLT1 leukotriene B4 receptor on the dorsal root ganglion neurons in mice.** *Brain Res Mol Brain Res* 2005, **137**:263-266.
24. Huang XJ, Zhang WP, Li CT, Shi WZ, Fang SH, Lu YB, Chen Z, Wei EQ: **Activation of CysLT receptors induces astrocyte proliferation and death after oxygen-glucose deprivation.** *Glia* 2008, **56**:27-37.
25. Caterina MJ, Schumacher MA, Tominaga M, Rosen TA, Levine JD, Julius D: **The capsaicin receptor: a heat-activated ion channel in the pain pathway.** *Nature* 1997, **389**:816-824.
26. Helliwell RJ, McLatchie LM, Clarke M, Winter J, Bevan S, McIntyre P: **Capsaicin sensitivity is associated with the expression of the vanilloid (capsaicin) receptor (VR1) mRNA in adult rat sensory ganglia.** *Neurosci Lett* 1998, **250**:177-180.
27. Dai Y, Moriyama T, Higashi T, Togashi K, Kobayashi K, Yamanaka H, Tominaga M, Noguchi K: **Proteinase-activated receptor 2-mediated potentiation of transient receptor potential vanilloid subfamily 1 activity reveals a mechanism for proteinase-induced inflammatory pain.** *J Neurosci* 2004, **24**:4293-4299.
28. Zhang H, Cang CL, Kawasaki Y, Liang LL, Zhang YQ, Ji RR, Zhao ZQ: **Neurokinin-1 receptor enhances TRPV1 activity in primary sensory neurons via PKCepsilon: a novel pathway for heat hyperalgesia.** *J Neurosci* 2007, **27**:12067-12077.
29. Hwang SW, Cho H, Kwak J, Lee SY, Kang CJ, Jung J, Cho S, Min KH, Suh YG, Kim D, Oh U: **Direct activation of capsaicin receptors by products of lipoxygenases: endogenous capsaicin-like substances.** *Proc Natl Acad Sci USA* 2000, **97**:6155-6160.
30. Thompson C, Cloutier A, Bosse Y, Poisson C, Larivee P, McDonald PP, Stankova J, Rola-Pleszczynski M: **Signaling by the cysteinyl-leukotriene receptor 2. Involvement in chemokine gene transcription.** *J Biol Chem* 2008, **283**:1974-1984.
31. Vulchanova L, Riedl MS, Shuster SJ, Stone LS, Hargreaves KM, Buell G, Surprenant A, North RA, Elde R: **P2X3 is expressed by DRG neurons that terminate in inner lamina II.** *Eur J Neurosci* 1998, **10**:3470-3478.
32. Burnstock G, Wood JN: **Purinergic receptors: their role in nociception and primary afferent neurotransmission.** *Curr Opin Neurobiol* 1996, **6**:526-532.
33. Dai Y, Fukuoka T, Wang H, Yamanaka H, Obata K, Tokunaga A, Noguchi K: **Contribution of sensitized P2X receptors in inflamed tissue to the**

mechanical hypersensitivity revealed by phosphorylated ERK in DRG neurons. *Pain* 2004, **108**:258-266.

34. Zhu WJ, Yamanaka H, Obata K, Dai Y, Kobayashi K, Kozai T, Tokunaga A, Noguchi K: **Expression of mRNA for four subtypes of the proteinase-activated receptor in rat dorsal root ganglia.** *Brain Res* 2005, **1041**:205-211.
35. Hamilton SG, McMahon SB, Lewin GR: **Selective activation of nociceptors by P2X receptor agonists in normal and inflamed rat skin.** *J Physiol* 2001, **534**:437-445.
36. Kobayashi K, Yamanaka H, Fukuoka T, Dai Y, Obata K, Noguchi K: **P2Y12 receptor upregulation in activated microglia is a gateway of p38 signaling and neuropathic pain.** *J Neurosci* 2008, **28**:2892-2902.
37. Yamanaka H, Obata K, Fukuoka T, Dai Y, Kobayashi K, Tokunaga A, Noguchi K: **Induction of plasminogen activator inhibitor-1 and -2 in dorsal root ganglion neurons after peripheral nerve injury.** *Neuroscience* 2005, **132**:183-191.
38. Chen ZL, Yoshida S, Kato K, Momota Y, Suzuki J, Tanaka T, Ito J, Nishino H, Aimoto S, Kiyama H, *et al*: **Expression and activity-dependent changes of a novel limbic-serine protease gene in the hippocampus.** *J Neurosci* 1995, **15**:5088-5097.
39. Yamanaka H, Obata K, Fukuoka T, Dai Y, Kobayashi K, Tokunaga A, Noguchi K: **Tissue plasminogen activator in primary afferents induces dorsal horn excitability and pain response after peripheral nerve injury.** *Eur J Neurosci* 2004, **19**:93-102.
40. Dai Y, Iwata K, Kondo E, Morimoto T, Noguchi K: **A selective increase in Fos expression in spinal dorsal horn neurons following graded thermal stimulation in rats with experimental mononeuropathy.** *Pain* 2001, **90**:287-296.

doi:10.1186/1744-8069-6-57
Cite this article as: Okubo *et al.*: Expression of leukotriene receptors in the rat dorsal root ganglion and the effects on pain behaviors. *Molecular Pain* 2010 **6**:57.

RESEARCH ARTICLE

Increase of Close Homolog of Cell Adhesion Molecule L1 in Primary Afferent by Nerve Injury and the Contribution to Neuropathic Pain

Hiroki Yamanaka, Kimiko Kobayashi, Masamichi Okubo, Tetsuo Fukuoka, and Koichi Noguchi*
Department of Anatomy and Neuroscience, Hyogo College of Medicine, Nishinomiya, Hyogo 663-8501, Japan

ABSTRACT

The L1 family of cell adhesion molecules (L1-CAMs) is known to be involved in various neuronal functions such as cell adhesion, axon guidance, and synaptic plasticity. We investigated the detailed expression/changes of a close homolog of the L1 cell adhesion molecule (CHL1) after nerve injury and the possible role on neuropathic pain using the rat spared nerve injury (SNI) model. SNI induced the expression of CHL1 in L4/5 DRG neurons, particularly in small-size injured neurons and in satellite cells. In the spinal cord, CHL1 immunoreactivity increased mainly in laminae I–II of the dorsal horn on the side ipsilateral to the nerve injury. Ultrastructural study clarified the fine localization of CHL1 in axons of primary afferents in the dorsal horn. CHL1 immunoreactivities were localized in the adherence such as axon–axon, axon–dorsal horn neurons (dendrite, soma), and axon–glial cells (astrocyte and microglia). Experimental inhibition of CHL1 adhesion by intrathecal administration of the antibody for CHL1 extracellular domain significantly prevented and reversed SNI-induced mechanical allodynia. Thus, alterations of CHL1 may be involved in the structural plasticity after peripheral nerve injury and have important roles in neuropathic pain. J. Comp. Neurol. 519:1597–1615, 2011.

INDEXING TERMS: dorsal root ganglia; peripheral nerve injury; synaptic reorganization; plasticity

Peripheral nerve injury often results in neuropathic pain with hyperalgesia and allodynia (Zimmermann, 2001), which is associated with hyperexcitability in the damaged dorsal root ganglion (DRG) neurons and alterations in pain signal modulatory mechanisms in spinal dorsal horn (DH) neurons (McLachlan et al., 1993; Stucky et al., 2001; Ji et al., 2003; Hains et al., 2004; Salter, 2005; Woolf, et al., 2007). Although numerous putative mechanisms have been implicated in neuropathic pain, the key mechanisms that control its induction and maintenance remain unclear. One general concept is that nerve injury induces a series of neuronal changes that recapitulate events during development (Chen et al., 2007), such as the neurite outgrowth or promotion of synapse formation. Several lines of evidence have indicated that peripheral nerve injury is associated with synaptic structural plasticity within the neuropil in lamina II of the dorsal horn. Such morphological plasticity includes synaptic and terminal degeneration of certain C-fiber afferents (Knyihar and Csillik, 1976; Kapadia and LaMotte, 1987), as well as sprouting and regeneration of synaptic contacts (Csillik and Knyihar, 1975; Wang et al., 2007).

L1 neural cell adhesion molecules (L1-CAMs) are immunoglobulin-class recognition proteins that promote axon growth and migration in developing neurons (Maness and Schachner, 2007). A close homolog of L1 (CHL1) is the most recently identified member of the L1 family. Its amino acid sequence is 60% identical to L1 in the extracellular region and 40% identical in the cytoplasmic domain (Holm et al., 1996). CHL1 is a strong promoter of neurite outgrowth in vitro and may bind to CHL1 homophilically as well heterophilically (Hillenbrand et al., 1999). During brain development, CHL1 is first expressed

Grant sponsor: Japanese Ministry of Education, Science, and Culture; Grant number: Grants-in-Aid for Scientific Research (ID 08105211), and a Pain Research Group Grant, Hyogo College of Medicine.

*CORRESPONDENCE TO: Koichi Noguchi, MD, PhD, Department of Anatomy and Neuroscience, Hyogo College of Medicine, Mukogawa-cho, Nishinomiya, Hyogo 663-8501, Japan. E-mail: noguchi@hyo-med.ac.jp

Received December 21, 2009; Revised June 22, 2010; Accepted December 14, 2010
DOI 10.1002/cne.22588
Published online December 23, 2010 in Wiley Online Library (wileyonlinelibrary.com)

at time of neurite outgrowth and the expression of CHL1 exhibits layer-specific pattern in the developing neocortex. The strong expression of CHL1 remains in the hippocampus at the adult stage (Hillenbrand et al., 1999). CHL1 knockout mice display aberrant guidance of olfactory axons and hippocampal mossy fibers, and these mice are defective in cognitive processing of spatial information (Montag-Sallaz et al., 2002) and attention (Pratte et al., 2003).

Given these molecular characteristics, biological activities, and developmental expression patterns, it is reasonable to propose that CHL1's ability to strengthen cell interactions could contribute to the reorganization of terminals in the dorsal horn following peripheral nerve injury. In the present study we test this hypothesis using a well-characterized spared nerve injury (SNI) model of neuropathic pain (Decosterd and Woolf, 2000) which also produces allodynia (increased sensitivity to innoxious stimuli) in the rat.

MATERIALS AND METHODS

Animal treatment

A total of 106 Male Sprague–Dawley rats (Nihon Doubutu, Osaka, Japan) weighing 200–250 g were used. All animal experimental procedures were approved by the Hyogo College of Medicine Committee on Animal Research and were carried out in accordance with the guidelines of the National Institutes of Health on animal care. Animals were anesthetized with sodium pentobarbital (50 mg/kg, intraperitoneally [i.p.]) and the tibial and common peroneal nerves were transected, while the sural nerve was left intact (spared nerve injury; SNI model). The wounds were then closed and the rats were allowed to recover. In the sham operation the procedures were the same except the nerves were only exposed and not transected. At several timepoints (1, 3, 7, 14 days) following the surgery, groups of rats were processed for analysis. Every effort was made to minimize animal suffering and reduce the number of animals used.

Intrathecal administration of anti-CHL1 antibody

After the SNI, the L6 vertebra was laminectomized and a soft tube (Silascon, Kaneka Medix, Osaka, Japan; outer diameter, 0.64 mm) filled with 5 μL of saline was inserted into the subarachnoid space for ≈0.5 cm length. After the muscle incision was closed, the mini-osmotic pumps (Alzet model 2001, Cupertino, CA) filled with nonimmune goat IgG (50 μg/mL) diluted in saline or goat polyclonal antibody against the CHL1 extracellular domain (R&D Systems, Minneapolis, MN) were connected to the tube. The concentrations of anti-CHL1 antibody were 5 or 50 μg/mL diluted in saline ($n = 6$ for behavioral analysis at each drug condition). Then the pump was laid under the skin and the incision was closed. The tube is held to the L6 spinous process and to back muscle using 4-0 nylon surgical sutures. The pump was implanted at least 24 hours before the first testing and the connection between pump and spinal cord was confirmed at the end day of behavioral analysis session.

Reverse transcription-polymerase chain reaction (RT-PCR)

For RT-PCR the rats were killed by decapitation under deep anesthesia with sodium pentobarbital (70–80 mg/kg body weight, i.p.) at 0, 3, 7, and 14 days after surgery, and the left L4, 5 DRG were removed and rapidly frozen with powdered dry ice and stored at −80°C until ready for use ($n = 4$ each timepoint). The procedure of extraction of total RNA using an RNA extraction reagent ISOGEN (Nippon Gene, Tokyo, Japan) was described in our previous study (Fukuoka et al., 2001). PCR primers for CHL1 and glyceraldehyde 3-phosphate dehydrogenase (GAPDH) cDNA were designed as follows: CHL1 primers (accession number XM001077843, 1647-2146), sense 5′-CCCCTTGAAGGTGGTCGGTAT-3′ and antisense 5′-GGA CAGCCGGACACTCCTGTT-3′; GAPDH primers (accession number M17701, 80-350), sense 5′-TGCTGGTGCTGAGT ATGTCG-3′ and antisense 5′-GCATGTCAGATCCACAA CGG-3′. The subsequent PCR reaction was performed with a standard method (Yamanaka et al., 2004).

Histological analysis

Rats that received SNI (0, 1, 3, 7, and 14 days, $n = 4$ at each timepoint) were deeply anesthetized with sodium pentobarbital (70–80 mg/kg body weight, i.p.) and perfused transcardially with 100 mL of 1% paraformaldehyde in 0.1 M phosphate buffer (pH 7.4) (PB), followed by 500 mL of 4% paraformaldehyde in 0.1 M PB. The L4/5 DRG and spinal cord were dissected out and postfixed in the same fixative for 4 hours at 4°C, followed by immersion in 30% sucrose in 0.1 M PB at 4°C overnight. The tissue was frozen in powdered dry ice, cut on a cryostat at a 25μm thickness for the spinal cord, and 4 μm thickness for the DRG. The sections were processed for in situ hybridization and immunohistochemistry.

In situ hybridization (ISH)

The protocol for ISH was described in detail previously (Yamanaka et al., 2004). The clone (p-GEM T-easy; Promega, Madison, WI) containing a partial sequence corresponding to the coding regions of CHL1 (1647-2146, accession number XM001077843,) was prepared and alpha-35S UTP-labeled antisense and sense cRNA probes

TABLE 1.
Primary Antibodies

Antibody	Immunogen	Host	Code/clone	Dilution	Source
Close homolog of L1 (CHL1)	Mouse CHL1 extracellular domain (amino acid, 25–1,043)	Goat	AF2147 (lot VEX015041)	(IHC 1:10000) (WB 1:2000)	R&D Systems
Activating transcription factor 3 (ATF3)	Peptide (194–212) of Human ATF3	Rabbit	C-19 (lot A256)	(IHC 1:1000) (WB 1:1000)	Santa Cruz Biotechnology
Neurofilament 200 (NF200)	C-terminus tail of H-subunit of pig neurofilament	Mouse	N0142/N52 (lot 028H4836)	(IHC 1:20000) (WB 1:5000)	Sigma
Glial fibrillary acidic protein (GFAP)	Cow spinal cord GFAP	Rabbit	Z334 (lot 096)	(IHC 1:5000) (WB 1:5000)	Dako
Microtubule associated protein 2 (MAP2)	Rat brain MAPs		M4403/HM-2 (lot 111K4806)	(IHC 1:5000) (WB 1:2500)	Sigma
Synaptophysin	Rat retina synaptophysin	Mouse	MAB368/SPV38 (lot 21071596)	(IHC 1:5000) (WB 1:5000)	CHEMICON
Growth associated protein 43 (GAP-43)	Rat GAP-43	Mouse	G-9264/GAP7B10 (lot 074H4822)	(IHC 1:10000) (WB 1:5000)	Sigma
Ionized calcium-binding adaptor molecule 1 (Iba1)	C-terminus of Iba1(N'-PTGPPAKKAISELP-C')	Rabbit	019-19741 (lot YNL3901)	(IHC 1:2500) (WB 1:500)	Wako

were synthesized using the enzyme-digested clones. The 35S-labeled probes in hybridization buffer were placed on the tissue sections on slides. The sections were incubated at 55°C overnight, then washed and treated with 1 μg/mL RNase A. Next the sections were air-dried. After the hybridization reaction the slides were coated with NTB emulsion (Kodak, Rochester, NY) and exposed for 2–5 weeks. Once developed in D-19 (Kodak), the sections were stained with hematoxylin-eosin and coverslipped. For double staining of CHL1 mRNA with activating transcription factor 3 (ATF3) or CHL1, sections were processed for immunohistochemistry using the ABC method (Yamanaka et al., 2004). After visualization of ATF3-immunoreactive (ir) or CHL1-ir, the sections were processed for ISH.

Immunohistochemistry (IHC)

The sections were processed for IHC as described before (Yamanaka et al., 2004). In brief, DRG and spinal cord sections were incubated with an antibody for single labeling or a mixture of two primary antibodies (Table 1) in Tris-buffered saline pH 7.4 (TBS) overnight at 4°C and followed by a mixture of Alexa Fluoro 488 or 594 conjugated secondary antibodies (1:5,000; Molecular Probes, Eugene, OR) overnight at 4°C. Finally, sections were incubated with a Hoechst 33342 (1:10,000; Molecular Probes) in order to stain the nuclei. Biotinylated antibody (Vector Laboratories, Burlingame, CA) was used as the secondary antibody for the ABC method. The resultant immunoperoxidase complexes were developed by incubation in 3,3-diaminobenzidine tetrahydrochloride (DAB) (Sigma, St. Louis, MO) and 0.01% hydrogen peroxidase.

Antibodies

Commercial antibodies against CHL1 and marker antigens were used. Table 1 provides information about these antibodies (commercial source, product number, and dilution) used in this study.

CHL1

Anti-mouse CHL1 antibody was raised against recombinant mouse CHL1 extracellular domain. It stained a single band at 200 kDa on western blots from rat spinal cord and DRG homogenates (Figs. 2, 4). A preabsorption control with the recombinant CHL1 was performed to test the specificity of the anti-mouse CHL1 antibody. The DRG sections of SNI model rats were processed for preabsorption test using the ABC method. Anti-mouse CHL1 antibody was incubated with the recombinant mouse CHL1 (Ala 25 – Gln 1043, R&D Systems) that was used to generate the antibody. Dilutions of 1:10,000 (CHL1 antibody, final concentration: 0.02 μg/mL) and 1:10 for the recombinant mouse CHL1 (final concentration: 2 μg/mL) were used in this study.

Activating transcription factor 3 (ATF3)

Anti-ATF3 antibody was used to identify injured DRG neuron (Tsujino et al., 2000). The staining pattern of ATF3 immunoreactivity (ir) was identical to our previous study (Tsujino et al., 2000). It recognized a single band at 21 kDa on western blots from rat DRG homogenate (Fig. 3M).

Neurofilament 200 (NF200)

Anti-NF200 antibody was used for the marker of the myelinated neuron (Lawson and Waddell, 1991;

Yamanaka et al., 2007a). The staining pattern of anti-NF200 antibody was identical to the previous studies (Jin et al., 2003; Anna et al., 2009; Clark et al., 2009). The antibody recognized a single band at 200 kDa on western blots from the rat spinal cord homogenate (Fig. 3N).

Glial fibrillary acidic protein (GFAP)

Anti-GFAP antibody was used for the marker of the satellite cell and astrocyte that was activated by peripheral nerve injury (Chudler et al., 1997; Yamanaka et al., 2007b). The staining pattern of anti-GFAP antibody in DRG and spinal cord was identical to the previous studies (Chudler et al., 1997; Ma and Quirion, 2002). It recognized a single band at 51 kDa on western blots from rat DRG homogenate (Fig. 3O).

Microtubule associated protein 2 (MAP2)

Anti-MAP2 antibody was used for the marker of the dendrite and neuronal cell body. The staining pattern of anti-MAP2 antibody in spinal cord was identical to the previous studies (Yamanaka et al., 2007a; Suzuki-Yamamoto et al., 2009). The antibody recognized a band at 280 kDa corresponded with a molecular weight of MAP2 on western blots from the rat spinal cord homogenate (Fig. 5I).

Synaptophysin

Anti-synaptophysin antibody was used for the marker of presynaptic terminal (Yamanaka et al., 2007a). The staining pattern of anti-synaptophysin antibody in the dorsal horn was identical to previous studies (Li et al., 2003). The antibody recognized a single band at 38 kDa on western blots from the rat spinal cord homogenate (Fig. 5J).

Growth-associated protein 43 (GAP-43)

Anti-GAP-43 antibody was used to identify the subpopulation of primary afferent that received injury in the dorsal horn of spinal cord (Woolf et al., 1990; Chong et al., 1994; Yamanaka et al., 2007a). Monoclonal GAP-43 was produced from hybridoma cells (clone GAP7B10). The staining pattern of anti-GAP-43 antibody in the dorsal horn was identical to previous studies (Woolf et al., 1990; Chong et al., 1994). The antibody recognized a single band at 43 kDa on western blots from the rat spinal cord homogenate (Fig. 6H).

Ionized calcium-binding adaptor molecule 1 (Iba1)

Anti-Iba1 antibody was used for the marker of the microglia that was activated by peripheral nerve injury (Yamanaka et al., 2007b; Kobayashi et al., 2008). It recognized a single band at 17 kDa on western blots from rat spinal cord homogenate (Fig. 8M). The staining pattern of anti-Iba1 antibody in the spinal cord was identical to previous studies in the spinal cord of peripheral nerve injury model rats (Narita et al., 2006; Romero et al., 2008).

Ultrastructural analysis of CHL1 in the dorsal horn

To investigate the ultrastructure of CHL1-ir profiles, the rats received peripheral nerve injury (14 days after SNI, $n = 4$) were anesthetized and perfused first with 100 mL of saline followed by 500 mL of 4% paraformaldehyde / 0.05% glutaraldehyde in PB. The spinal cord was immediately removed and placed in the same fixative for 24 hours. Serial frontal sections were cut at 50 μm with a vibratome. The sections were rinsed with TBS and incubated with a TBS containing 5% normal horse serum (NHS) for 30 minutes. After rinsing with the washing buffer, the sections were incubated with goat polyclonal antibody against the CHL1 extracellular domain (1:2,500, R&D Systems) in the washing buffer containing 5% NHS for 3 days. The sections were washed in TBS and then incubated in biotinylated antigoat IgG (1:400; Vector Laboratories) containing 5% NHS for 24 hours, followed by incubation in avidin-biotin-peroxidase complex (Elite ABC kit; Vector) for 30 minutes at room temperature. The hydrogen peroxidase reaction was developed in TBS containing 0.05% DAB (Wako, Tokyo, Japan) and 0.01% hydrogen peroxidase. Sections were then washed in TBS. After rinsing with PB, the sections were postfixed with 2% OsO_4 in PB for 2 hours. The sections were then dehydrated and embedded between Aclar films (Nisshin EM, Tokyo, Japan) with Epon 812. After confirming the presence of the CHL1-ir neurons, laminae I-II of the dorsal horn were trimmed under microscopic observation. Ultrathin sections were made and collected on Formvar-coated single-slot grids. Then the sections were stained with uranyl acetate and Reynold's solution and examined with a H7100 transmission electron microscope (Hitachi, Tokyo, Japan). All incubations and washes were carried out at room temperature. The CHL1-ir profiles were sampled randomly and photographed at a final magnification of 5,000–10,000×.

Western blot analysis (WB)

For the WB analysis the rats were killed by decapitation under deep anesthesia at 0, 3, and 14 days after SNI ($n = 4$ each timepoint) and the ipsilateral L4/5 DRG and spinal cord were removed and rapidly frozen with powdered dry ice. Frozen spinal cord was homogenized (Polytron PT3000, Brinkmann Instruments, Westbury, NY) at 10% (w/v) in a modified buffer containing 20 mM Tris-HCl, pH 7.4, 10% sucrose, and protease inhibitors (Protease inhibitor cocktail, 1:5,000;

Nakarai, Kyoto, Japan). Homogenates were vortexed for 60 minutes with intervening cooling and centrifuged for 60 minutes at 14,000 rpm at 4°C to recover the supernatant. Proteins were resolved using 10% sodium dodecyl sulfate-polyacrylamide gel electrophoresis (SDS-PAGE) and 15 μg of protein was applied to each lane. After electrophoresis, proteins were transferred onto PVDF membranes (Immobilon-P, Millipore, Bedford, MA) in 25 mM Tris/200 mM glycine for 100 minutes at 100 mA. Blots were blocked for 1 hour in 10% fat-free milk in 0.1 M Tris-buffered saline containing 0.05% Tween 20. Incubations with primary antibodies were performed overnight at 4°C. Secondary antibodies, IgG conjugated to alkaline phosphatase, were incubated for 1 hour at room temperature. Signal was detected by chemiluminescence using CSPD ready-to-use reagent (Roche, Indianapolis, IN). Films were scanned and quantified using the NIH Image system, v. 1.61 (Bethesda, MD).

Quantification

Quantification of ISH was performed as described before (Yamanaka et al., 2004). All neurons in two nonserial L4/5 DRG sections that contained at least 400 neurons with visible nuclei were used for quantification of signal intensity. These two nonserial sections were separately corrected from one DRG at a distance of more than 200 μm. For image analysis of the sections processed for ISH, we analyzed the density of silver grains over all neuronal profiles containing nuclei in the selected sections using a computerized image analysis system (NIH Image v. 1.61). At a magnification of 200× and with brightfield illumination, the upper and lower thresholds of gray level density were set such that only silver grains were accurately discriminated from the background in the outlined cell or tissue profile and read by the computer pixel-by-pixel. Next, the area of discriminated pixels was measured and divided by the area of the outlined profile, giving a grain density for each cell or tissue profile. To reduce the risk of biased sampling of the data owing to varying emulsion thickness, the percentage of grain-occupied area of each neuronal profile was divided by the background grain density giving a signal/noise (S/N) ratio. The S/N ratio of an individual neuron and its cross-sectioned area, which was computed from the outlined profile, were plotted as shown in Figure 1G,H. Based on these scattergrams, none of the sections hybridized with sense probes revealed a significant accumulation of silver grains in any regions of the tissue (data not shown). At least 400 neurons from the L4/5 DRG of each rat were measured.

Photomicrographs

All images from the ISH and double labeling of ISH and IHC with DAB staining were digitized with a Nikon DIAPHOT-300 microscope (Nikon, Japan) connected to a Nikon DXM-1200 digital camera (Nikon, Japan). Double or triple staining 2D images were acquired using a confocal laser scanning microscope (model LSM 510 v. 2.8; Carl Zeiss Microimaging, Germany) with the oil Plan-Neofular 40× and 100× objective lens. We used Adobe Photoshop 6.0 (Adobe Systems, Mountain View, CA) to optimize the images and to make all figures.

Behavioral tests

All SNI rats were tested for mechanical allodynia and hyperalgesia of the plantar surface of the hindpaw 1 day before surgery and 0, 3, 5, 7, 9, 12, and 14 days after surgery. Mechanical allodynia was assessed with a dynamic plantar aesthesiometer (Ugo Basile, Comerio, Italy), which is an automated von Frey-type system (Kalmar et al., 2003; Lever et al., 2003). To measure mechanical thresholds of the hindpaw, rats were placed in a plastic cage with a wire mesh floor and allowed to acclimate for 15 minutes before each test session. A paw-flick response was elicited by applying an increasing force (measured in grams) using a plastic filament (0.5 mm diameter) focused on the lateral of the plantar surface of the ipsilateral hindpaw (sural nerve territory). The force applied was initially below the detection threshold, then increased from 1 to 50 g in 1-g steps over 20 seconds, and was then held at 50 g for an additional 10 seconds. The rate of force increase was 2.5 g/sec. The force required to elicit a reflex removal of the ipsilateral hindpaw was monitored. This was defined as the mean of three measurements made at 5-minute intervals. Data are expressed as mean ± SEM. Differences of values over time of each group were tested using one-way analysis of variance (ANOVA), followed by individual post-hoc comparisons (Fisher's PLSD). Pairwise comparisons (Student's *t*-test) were used to assess the effect of the CHL1 antibody on the basal mechanical sensation. A difference was accepted as significant if $P < 0.05$.

RESULTS

Expression of CHL1 mRNA in the DRG

To examine whether CHL1 mRNA level is upregulated in response to the sciatic nerve injury, we performed RT-PCR using the total RNA extracted from L4 and L5 DRGs on the side ipsilateral to the injury (Fig. 1A). The intensity of amplified band of CHL1 was increased as early as 3 days following the sciatic nerve injury, rising to double of the constitutive expression levels (213.5 ± 25.3%, $P < 0.01$, $n = 4$). The significant increase remained for 2 weeks following the peripheral nerve injury. Expression of CHL1 mRNA at the cellular level was examined by ISH. In the control, 45% of the total neurons expressed CHL1

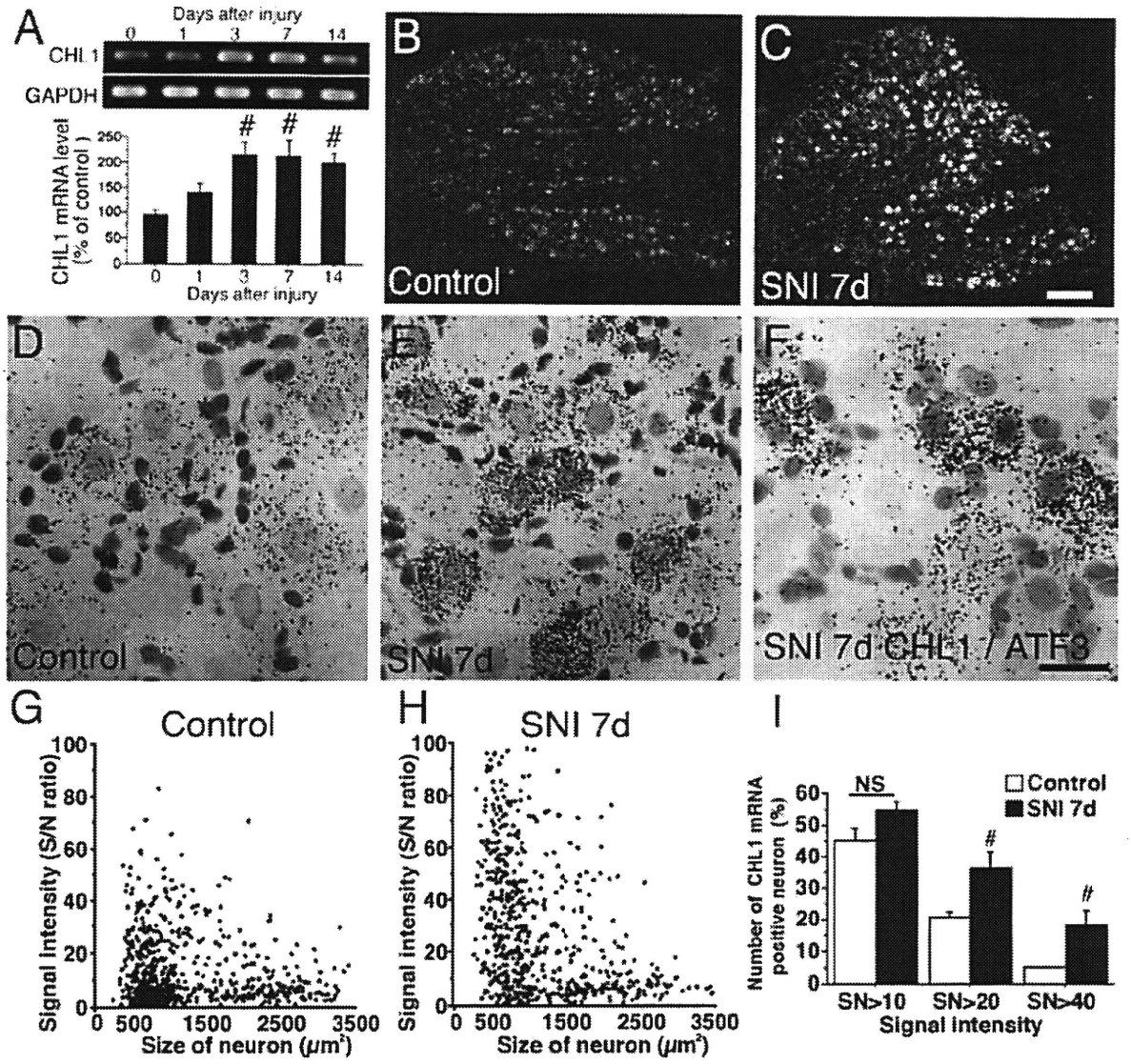

Figure 1. Expression of CHL1 mRNA in L4, 5 DRG after SNI. **A:** The levels of CHL1 mRNA in the ipsilateral L4, 5 DRG were determined by the RT-PCR technique. Gel panels show PCR products from the L4, 5 DRG taken at 1, 3, 7, and 14 days after surgery ($n = 4$ at each timepoint). Graph shows the mRNA levels of CHL1 expressed as percentages of the mRNA level in the normal control ganglia (mean ± SEM). #Significant compared with the naive control ($P < 0.05$; ANOVA). **B,C:** Darkfield images of ISH showing CHL1 mRNA in the L5 DRG of a control rat (B) and 7 days after SNI (C). **D,E:** Brightfield images of the ISH for CHL1 mRNA in the control (D) and ipsilateral DRG at 7 days after SNI (E). **F:** Double labeling of ISH for CHL1 mRNA and ATF3-ir in the ipsilateral L5 DRG at 7 days after SNI. **G,H:** Scatterplot diagrams of CHL1mRNA expression in the injured (7 days) and control L4 and L5 DRG ($n = 4$, total 2,299 neurons for SNI, total 2,322 neurons for control naive). Individual cell profiles are plotted according to the cross-sectional area (along x-axis) and S/N ratio (along the y-axis). **I:** Quantification of the number of CHL1 mRNA expressing neurons in the injured and control DRG. NS indicates not significant compared with control and #significant compared with the naive control ($P < 0.05$; Student's *t*-test). The sections were stained with hematoxylin-eosin (D,E) or hematoxylin (F). Scale bars = 250 μm in B,C; 25 μm in D–F.

mRNA (Fig. 1B,D). SNI clearly increased the CHL1 mRNA signals in the ipsilateral DRG (Fig. 1C,E). Hybridization signals were highly accumulated in small size neurons in the ipsilateral DRG and the high level signals were colocalized with ATF3-ir (Fig. 1F), the specific marker for injured DRG neurons (Tsujino et al., 2000). In control DRG, low levels of CHL1 mRNA were expressed in the nonneuronal cells such as satellite cells. After SNI we could detect the increase of grain accumulation in the ipsilateral nonneuronal cells. (Fig. 1C,E). Quantification of the silver grains on neuronal somata revealed that the signal intensity of the CHL1 mRNA was upregulated, particularly in

small-medium DRG neurons (Fig. 1G,H). SNI did not significantly increase the total number of the CHL1 mRNA-positive neurons (S/N ratio >10). Rather, it increased the transcriptional level in labeled neurons, given the substantial increase of cell number showing the high level (S/N ratio >20 or >40) of CHL1 mRNA (Fig. 1I).

Expression of CHL1 protein in the DRG

Expression of CHL1 protein was confirmed by WB analysis of the DRG using antibody against the CHL1 extracellular domain. As expected from the mRNA analysis (Fig. 1), the protein levels of CHL1 in the DRG were dramatically upregulated after peripheral nerve injury. WB analysis showed an increase of the 200 kDa single CHL1-ir band following SNI (Fig. 2A). At 3 days after SNI, CHL1 protein significantly increased and continued elevated until day 14 (Fig. 2A,B, $n = 4$ each timepoint). We examined the effect of SNI on the localization of CHL1 protein in the DRG by immunohistochemistry. In the control DRG, cytoplasmic CHL1-ir was at a low level (Fig. 2C). After nerve injury the CHL1-ir was increased in both cytoplasm of small to medium-sized DRG neurons and nonneuronal cells (Fig. 2D). We carried out two sets of control experiments (preabsorption experiment and double labeling analysis of ISH and IHC in DRG) to confirm the specificity of the antibody for CHL1. The results showed that the staining pattern of CHL1-ir by the ABC method was indeed consistent with the fluorescent immunostaining (Fig. 2E,F,H,I) and that no immunoreactivity was found in the preabsorption control sections (Fig. 2G). Double labeling analysis revealed that hybridization signals for CHL1 mRNA were specifically located on the CHL1-ir cells both in control and injured DRG (Fig. 2H,I).

Characterization of CHL1-ir cells in the DRG

In order to classify subtypes of cells showing upregulation of CHL1 following nerve injury (7 days after SNI), we used a variety of markers: activating transcription factor 3 (ATF3), injured DRG neuron (Tsujino et al., 2000), neurofilament 200 (NF200), a marker of myelinated afferents (Lawson and Waddell, 1991), and GFAP, which is expressed in satellite cell and Schwann cell (Chudler et al., 1997). Sections were processed for double labeling, followed by Hoechst 33342 labeling to stain nuclei. Triple labeling immunohistochemistry of CHL1 with ATF3 and Hoechst 33342 revealed that the cytoplasmic expression of CHL1 was upregulated exclusively in the ATF3-ir labeled injured neurons following SNI (Fig. 3A–D).

Neurons with intense labeling of CHL1-ir were negatively labeled for NF200, which was consistent with the ISH data. Only a small number of large-size neurons showed colocalization of CHL1-ir with NF200-ir (Fig. 3E–H). Upregulation of CHL1 in nonneuronal cells was observed in cells surrounding large-diameter ATF3-positive neurons (Fig. 3C). In satellite cells in the vicinity of large-size neurons, CHL1-ir was increased and colocalized with GFAP-ir (Fig. 3I–L). Taken together, peripheral nerve injury induced CHL1 mainly in small unmyelinated neurons that received injury and in satellite cells in the vicinity of the injured large size neurons in DRG.

Expression of CHL1 in the spinal cord following SNI

In the L4–5 spinal cord, the WB analysis revealed that SNI significantly increased CHL1 protein from 3 days and remained elevated for at least 14 days after injury (Fig. 4A,B). In situ hybridization of the L4–5 spinal cord did not show any changes in the intrinsic expression of CHL1 mRNA (Fig. 4C). In control rats, CHL1-ir in the spinal cord was predominantly localized in laminae I–II and appeared as fiber-like structures (Fig. 4D). SNI increased the CHL1-ir profiles in laminae I–II in the L4–5 spinal cord on the side ipsilateral to the injury (Fig. 4E,F). In the lower-magnification images, expression of CHL1-ir at 3 and 14 days after SNI seemed similar. However, high-power magnification confocal images demonstrated that CHL1-ir appeared as small varicosity-like structures in the control and the size of CHL1-ir profiles began to enlarge from 3 to 14 days after SNI (Fig. 4G–J).

Characterization of SNI induced CHL1-ir varicosities in the dorsal horn

Increase of CHL1 in injured small DRG neurons (Figs. 1–3) and the staining pattern of CHL1 in the dorsal horn after SNI (Fig. 4) strongly suggest that the CHL1-ir varicosities were terminals of primary afferents. We performed double labeling of CHL1 with MAP2, a marker of dendrite and neuronal somata, or with synaptophysin, a presynaptic marker. Confocal images of double labeling with CHL1 and MAP2 revealed that CHL1-ir varicosities were attached but not colocalized with MAP2-ir dendrites after SNI (Fig. 5A–C). Double labeling analysis of CHL1 with synaptophysin revealed a partial colocalization of CHL1-ir with synaptophysin in the ipsilateral dorsal horn (Fig. 5E–G). CHL1-ir varicosities were not completely filled by synaptophysin-ir but a number of CHL1-ir varicosities contained synaptophysin-ir. In contrast to the SNI, a very low level of CHL1 labeling was observed on the contralateral side and did not colocalize with these marker proteins (Figs. 5D,H).

In order to confirm that the SNI-induced CHL1-ir varicosities are the primary afferents in the dorsal horn, double labeling analysis of CHL1 with GAP-43 was performed because the peripheral nerve injury was known to induce GAP-43 in the DRG and its terminals in laminae I–II of the